ARTICLE

Cancer-derived sialylated IgG promotes tumor immune escape by binding to Siglecs on effector T cells

Zihan Wang[1,2,3], Zihan Geng[1,2,3], Wenwei Shao[1,2], Enyang Liu[1,2], Jingxuan Zhang[1,2], Jingshu Tang[1,2], Pingzhang Wang[1,3], Xiuyuan Sun[1,2], Lin Xiao[4], Weiyan Xu[1,2], Youhui Zhang[5], Heng Cui[6], Liang Zhang[7], Xi Yang[7], Xiaohong Chang[6] and Xiaoyan Qiu[1,2,3]

To date, IgG in the tumor microenvironment (TME) has been considered a product of B cells and serves as an antitumor antibody. However, in this study, using a monoclonal antibody against cancer-derived IgG (Cancer-IgG), we found that cancer cells could secrete IgG into the TME. Furthermore, Cancer-IgG, which carries an abnormal sialic acid modification in the CH1 domain, directly inhibited effector T-cell proliferation and significantly promoted tumor growth by reducing $CD4^+$ and $CD8^+$ T-cell infiltration into tumor tissues. Mechanistic studies showed that the immunosuppressive effect of sialylated Cancer-IgG is dependent on its sialylation and binding to sialic acid-binding immunoglobulin-type lectins (Siglecs) on effector $CD4^+$ and $CD8^+$ T cells. Importantly, we show that several Siglecs are overexpressed on effector T cells from cancer patients, but not those from healthy donors. These findings suggest that sialylated Cancer-IgG may be a ligand for Siglecs, which may serve as potential checkpoint proteins and mediate tumor immune evasion.

Keywords: IgG; Cancer-derived IgG; tumor microenvironment; sialylation; tumor immune escape

Cellular & Molecular Immunology (2020) 17:1148–1162; https://doi.org/10.1038/s41423-019-0327-9

INTRODUCTION

Although elevated immunoglobulin (Ig) levels in patients with cancer are believed to be the result of increased expression of B cell-derived antitumor antibodies, a growing body of evidence indicates that IgG in the tumor microenvironment (TME) usually has procancer activity by blocking either T-cell-mediated tumor cytotoxicity (once believed to be mediated by a molecule named "blocking factor") or proinflammatory activity.[1–3] Thus, B cells have been considered to play either antitumor or "rebel" roles in antitumor immunity. In fact, increasing evidence from our group and others indicates that IgG is overexpressed in many cancer cells.[4–7] Moreover, cancer-derived IgG (Cancer-IgG) that displays growth factor-like activity and promotes the progression of cancer cells can be produced.[4,8–11] These findings suggest that IgG in the TME includes Cancer-IgG and B cell-derived IgG (B-IgG) and that the "rebel" IgG may be derived from cancer cells.

Recently, we used a monoclonal antibody, RP215, which was developed by the Lee group in 1987, and found that RP215 can distinguish Cancer-IgG from B-IgG.[12,13] Unexpectedly, the epitope recognized by RP215 carries a unique sialic acid modification localized to a new N-glycosylation site, Asn162, in the CH1 domain of the IgG heavy chain[14] rather than the classic Asn297 site.[15] Cancer-derived sialylated IgG (SIA-CIgG) can directly promote cancer progression by binding to integrin α6β4 and activating integrin-FAK signaling. Evidently, RP215 shows strong anticancer activity.[14]

In recent years, it has been found that Ig can negatively regulate the T-cell-mediated immune response. IgG and IgA in colostrum can maintain immune homeostasis in the neonatal intestinal mucosa by inhibiting T-cell activation;[16] in addition, sialylated IgM has immunomodulatory effects on effector T cells.[17] Importantly, intravenous immunoglobulin (IVIG), which is widely used in the clinic, has anti-inflammatory effects. Mechanistic studies suggest that the anti-inflammatory effect of IVIG is dependent on a small fraction of IgG, in which the IgG Fc domain is modified by sialic acid.[15,18] However, the detailed mechanism needs to be investigated further.[19] Sialylated IgG in IVIG can indirectly inhibit dendritic cell (DC)- and macrophage-mediated $CD4^+$ T-cell activation by binding to the sialic acid receptor dendritic cell-specific ICAM-3 grabbing nonintegrin (DC-SIGN) on DCs.[20–22] Siglecs are a family of sialic acid receptors that comprise 15 members in humans, and most of these receptors mediate immune suppression. Inhibitory Siglecs are frequently expressed on some immune cells, such as myeloid cells, monocytes, DCs, NK cells, and B cells, and inhibit the activation of these immune cells.[23,24] Recently, growing evidence has shown that Siglecs, including Siglec-3, Siglec-7, Siglec-9, and Siglec-10, are also expressed on effector T cells.[25–32] In addition, mouse Siglec-E, Siglec-F, and Siglec-G have also been reported to be expressed on T cells.[30,33] Based on these observations, we hypothesized that SIA-CIgG is involved in tumor immune escape by binding to sialic acid receptors on immune cells.

[1]Department of Immunology, School of Basic Medical Sciences, Peking University, Beijing 100191, China; [2]NHC Key Laboratory of Medical Immunology, Peking University, Beijing 100191, China; [3]Key Laboratory of Molecular Immunology, Chinese Academy of Medical Sciences, Beijing 100191, China; [4]Department of Clinical Laboratory, National Cancer Center/Cancer Hospital, Chinese Academy of Medical Sciences and Peking Union Medical College, Beijing 100021, China; [5]Department of Immunology, Cancer Institute & Hospital, Chinese Academy of Medical Science, Beijing 100021, China; [6]Gynecologic Oncology Center of Peking University Peoples' Hospital, Beijing 100044, China and [7]Key Laboratory of Biochip Technology, Biotech and Health Centre, Shenzhen Research Institute of City University of Hong Kong, Shenzhen, Guangdong 518057, China
Correspondence: Xiaohong Chang (changxiaohong@pkuph.edu.cn) or Xiaoyan Qiu (qiuxy@bjmu.edu.cn)
These authors contributed equally: Zihan Wang, Zihan Geng.

Received: 3 March 2019 Accepted: 21 October 2019
Published online: 21 November 2019

In this study, we first found that SIA-CIgG could inhibit T-cell proliferation and promote tumor growth by inducing reductions in $CD4^+$ and $CD8^+$ T-cell frequencies in tumor tissues. Mechanistically, SIA-CIgG, which depends on sialylation of the novel CH1 domain but not the classic CH2 domain, directly bound to Siglecs, such as Siglec-7 and Siglec-10, on effector $CD4^+$ and $CD8^+$ T cells, inhibiting T-cell proliferation and promoting tumor growth. Importantly, we found that Siglecs, such as Siglec-3, Siglec-6, Siglec-7, and Siglec-10, were expressed at significantly higher levels on $CD4^+$ and $CD8^+$ T cells from patients with cancer than on those from healthy donors. These findings reveal that SIA-CIgG may be a novel ligand for sialic acid receptors, and that the Siglecs expressed on effector T cells are potential immune checkpoint molecules.

RESULTS

IgG containing Cancer-IgG in the TME can directly suppress $CD4^+$ and $CD8^+$ T-cell proliferation

RP215 recognizes Cancer-IgG, which was found to be widely expressed in epithelial cancer cells, such as breast, liver, lung, and colon cancer cells, especially in the cancer stem cell populations.[4,14,34,35] The expression of RP215-recognized Cancer-IgG directly indicates a poor prognosis in patients with one of several epithelial carcinomas, such as breast cancer,[35] bladder cancer, salivary gland cystadenocarcinoma,[36] non-small cell lung cancer,[14,37] and renal cell carcinoma.[38] Moreover, recognition by RP215 depends on a novel N-glycosylation site-related sialylated epitope located in CH1 (Asn162) of the Cancer-IgG heavy chain,[14] which is distinct from the classic N-glycosylation site located in CH2 (Asn297)[15] (Fig. 1a). Therefore, we first identified SIA-CIgG in the TME of various cancers, including breast cancer and ovarian cancer, by immunohistochemistry using RP215 and found a large amount of SIA-CIgG deposition in the TMEs (Fig. 1b). Next, we purified IgG with protein G and found a high proportion of RP215-recognized IgG in the IgG purified from the TME (TME-IgG) by Western blotting. In contrast, a commercial anti-human IgG antibody, which mainly recognizes circulating IgG, recognized both TME-IgG and IVIG (Fig. 1c–e). These results suggest that there is a large amount of SIA-CIgG in the TME. Furthermore, SIA-CIgG carries a unique sialic acid modification; therefore, RP215 can be used to distinguish SIA-CIgG from B-IgG.

Currently, IVIG is widely used in the treatment of autoimmune diseases and many inflammatory diseases. Mechanistically, IVIG, which is dependent on its 1–5% sialylated IgG content,[15,39,40] can directly bind to the sialic acid receptor DC-SIGN on DCs or macrophages, decreasing the activity of the DCs or macrophages and thus indirectly inhibiting $CD4^+$ T-cell activation mediated by the DCs or macrophages.[20–22,41] To confirm the immunomodulatory effect of TME-IgG, which contains a high proportion of SIA-CIgG, TME-IgG was first purified by protein G and then used to treat peripheral blood mononuclear cells (PBMCs), including lymphocytes, monocytes, and DCs, isolated from healthy donors. These cells were labeled with carboxyfluorescein succinimidyl ester (CFSE) and stimulated with anti-CD3 and anti-CD28 mAbs, and the proliferation of $CD4^+$ and $CD8^+$ T cells was measured after 72 h. As expected, the proliferation of $CD4^+$ and $CD8^+$ T cells was markedly inhibited by TME-IgG in a dose-dependent manner. However, IVIG showed a weaker immunomodulatory effect on T-cell proliferation than TME-IgG (Supplementary Fig. S1a). To determine whether the inhibitory effect of TME-IgG is myeloid cell dependent, we treated peripheral blood lymphocytes (PBLs) with TME-IgG or IVIG and stimulated these cells with anti-CD3 and anti-CD28 mAbs in the absence of myeloid cells. Unlike those of previous reports,[20–22,41] the results in this study clearly showed that TME-IgG retained its inhibitory effects on T-cell proliferation; similarly, the inhibitory effect of TME-IgG was stronger than that of IVIG (Supplementary Fig. S1b). Accordingly, the levels of the Th1 cytokines IL-2, IFN-γ, and TNF-α and the Th2 cytokines IL-4 and IL-10 were significantly decreased in culture supernatants after treatment with 50 μg/ml TME-IgG (Supplementary Fig. S1c), which suggested that TME-IgG could directly inhibit T-cell proliferation. IL-6 levels were not changed by the addition of TME-IgG or IVIG. Subsequently, $CD4^+$ and $CD8^+$ T cells were sorted by flow cytometry. As expected, TME-IgG exhibited a significant inhibitory effect on the proliferation of sorted $CD4^+$ or especially $CD8^+$ T cells that was dose dependent (Fig. 1f, g). It is worth noting that no obvious inhibitory effect or dose-dependent effect of TME-IgG on the proliferation of sorted B cells stimulated by staphylococcal protein A was observed (Supplementary Fig. S1d). These results demonstrate that IgG in a TME containing Cancer-IgG can directly suppress $CD4^+$ and $CD8^+$ T-cell proliferation.

TME-IgG containing SIA-CIgG promotes tumor growth in mice in a manner dependent on reducing T-cell frequencies

To perform the necessary in vivo experiments, we first evaluated the immunosuppressive effects of both mouse TME-IgG and human TME-IgG on mouse T cells. We purified mouse TME-IgG from B16 and EMT-6 cancer tissue samples that were grown in B and T-cell-deficient $RAG1^{-/-}$ or NOD SCID mice. We found that both mouse TME-IgG and human TME-IgG significantly suppressed the proliferation of mouse T cells activated with anti-CD3 and anti-CD28 mAbs or ConA (Supplementary Fig. S2a–c). These results suggest that both human and mouse TME-IgG have immunosuppressive effects on mouse T-cell proliferation. Importantly, human TME-IgG has cross-species immunosuppressive effects on mouse T cells; thus, it is reasonable that human TME-IgG can be used in place of mouse TME-IgG.

Next, we first established a mouse melanoma model in C57BL/6 mice (Fig. 2a), in which human TME-IgG or IVIG (as a control) was injected subcutaneously into the peritumoral area, and the progrowth effects of these treatments were monitored by measuring tumor size. TME-IgG significantly promoted tumor growth, whereas IVIG had no influence on tumor growth (Fig. 2b–d). Notably, the numbers of $CD4^+$ and $CD8^+$ T cells in the draining lymph nodes (DLNs) of the mice significantly decreased after treatment with TME-IgG (Fig. 2e).

To determine whether the protumor effect of TME-IgG was dependent on T cells, we performed the same experiments in T-cell-deficient nude mice. The results showed that the TME-IgG-treated mice exhibited no protumor effect compared with wild-type mice (Fig. 2f–h). To analyze whether TME-IgG can directly promote the proliferation of B16 cells, TME-IgG or IVIG was used to treat B16 cells in vitro for 3 days, and the proliferation of the B16 cells was assessed by a CCK8 assay. The results suggested that neither TME-IgG nor IVIG directly promoted the proliferation of B16 cells in vitro in the absence of immune cells (Supplementary Fig. S2d). Thus, both the in vivo and in vitro results provide evidence that the protumor effect of TME-IgG is dependent on a reduction in the effector T-cell frequency induced by TME-IgG.

SIA-CIgG but not B-IgG can directly inhibit proliferation and reduce effector T-cell frequencies in vitro and in vivo

To exclude the possibility that TME-IgG contains B-IgG, we utilized an affinity column coupled with RP215 to purify SIA-CIgG from TME-IgG, as described previously,[14] and the inhibitory effect of SIA-CIgG on T-cell proliferation was also measured, as described above. Compared with the nonbinding IgG fractions, the SIA-CIgG fraction significantly inhibited T-cell proliferation, especially $CD8^+$ T-cell proliferation (Fig. 3a, b).

Subsequently, in accordance with our previous findings, we produced recombinant Cancer-IgG with $V_H5\text{-}51/D3\text{-}9/J_H4$ (GenBank: AY270190.1) heavy chains and $V_κ4\text{-}1/J_κ3$ (GenBank: AY505537.1) light chains, which are widely expressed by many epithelial cancer cells, such as lung cancer, breast cancer, colon cancer, and oral carcinoma cells.[4] As expected, our results showed

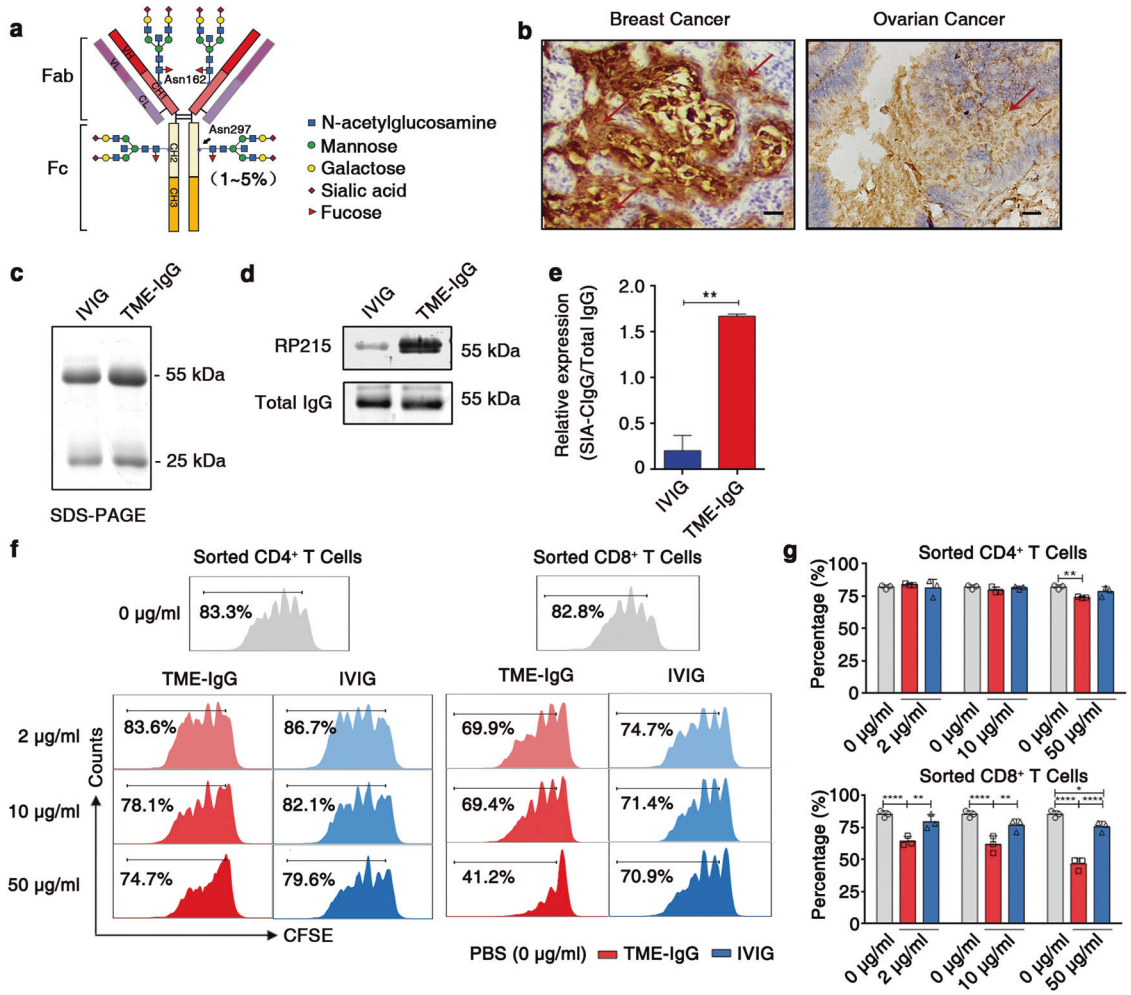

Fig. 1 Purified TME-IgG containing abundant SIA-CIgG can directly inhibit T-cell proliferation. **a** The structure of the sugar moiety that is linked to the Fc fragment of intravenous immunoglobulin (IVIG) with enhanced anti-inflammatory activity. The structures of sialylated N-glycans located at the Asn162 site of SIA-CIgG Fab fragments and classic sialylated N-glycans attached to Asn297 in IgG Fc fragments are shown. Variable residues such as N-acetylglucosamine (blue square), mannose (green circle), galactose (yellow circle), sialic acid (purple diamonds), and fucose (red triangle) are shown. The classic sialylated N-glycans attached to Asn297 in IgG were present in ~1–5% of the total serum IgG pool. **b** Immunohistochemical staining for SIA-CIgG in the TME of human breast and ovarian cancer tissue samples using RP215. Scale bars, 100 μm. **c** Identification of purified TME-IgG using SDS-PAGE. IVIG was used as a control. **d** SIA-CIgG in TME-IgG detected by western blotting using RP215, and total IgG estimated by a commercial anti-IgG antibody. **e** Expression of SIA-CIgG relative to that of the total IgG evaluated as in (**d**) and calculated with the average gray value of three measurements for each band. **f** Proliferation of PBS-, TME-IgG-, and IVIG-treated $CD4^+$ and $CD8^+$ T cells. The doses of TME-IgG or IVIG were 0 μg/ml, 10 μg/ml, and 50 μg/ml. Cells were sorted by flow cytometry, labeled with carboxyfluorescein succinimidyl ester (CFSE), and then activated for 72 h using precoated 3 μg/ml anti-CD3 and 1 μg/ml anti-CD28 mAbs. **g** Proportion and statistical significance of proliferating $CD4^+$ and $CD8^+$ T cells sorted by flow cytometry and treated with TME-IgG or IVIG as in (**f**) ($n = 3$ each group). IVIG intravenous immunoglobulin, TME-IgG tumor microenvironment IgG. Small horizontal lines (**e, g**) indicate the mean (± s.d.). $^{*}P \le 0.05$, $^{**}P \le 0.01$, and $^{****}P \le 0.0001$ (two-tailed Student's *t* test for unpaired data). Data are from one experiment that was representative of three (**c**–**g**) independent experiments with similar results. Also see Supplementary Fig. S1.

that recombinant Cancer-IgG expressed in CHO cells could be recognized by RP215 (Supplementary Fig. S3a). More importantly, this recombinant SIA-CIgG (rSIA-CIgG) also had significant inhibitory effects on the proliferation of $CD4^+$ and $CD8^+$ T cells with or without myeloid cells (Fig. 3c–e).

To further examine the inhibitory effect of rSIA-CIgG in vivo, we also established B16 tumor model in C57BL/6 mice, and tumor growth and the proportion of immune cells in the tumor tissue or DLNs were evaluated. Similar to TME-IgG, rSIA-CIgG significantly promoted tumor growth (Fig. 3f–h) and markedly decreased $CD8^+$ T-cell frequencies in both tumor tissue (Fig. 3i) and the DLNs (Fig. 3j). Next, we established a mouse breast cancer EMT-6 model in BALB/c mice and treated these mice with rSIA-CIgG. As seen in the B16 model mice, rSIA-CIgG showed significant protumor effects (Fig. 3k–m) and decreased $CD4^+$ and $CD8^+$ T-cell frequencies in both tumor tissue (Fig. 3n) and the DLNs (Fig. 3o). Together, these results suggest that the majority of TME-IgG is produced by cancer cells; moreover, SIA-CIgG can be involved in tumor immune escape by reducing the proportions of effector $CD4^+$ and $CD8^+$ T cells.

Inhibitory effect of SIA-CIgG on effector T cells is dependent on sialylation

To analyze the modification of SIA-CIgG with sialic acid, *Sambucus nigra* lectin (SNA), a lectin specific for α2,6 sialic acids, was used to determine the sialylation state of SIA-CIgG. Nearly 1–5% of IVIG was previously reported to be sialylated, and IVIG was used as a control.[18,39,40] As expected, TME-IgG displayed a higher level of sialylation than IVIG by western blotting using the lectin SNA (Fig. 4a). In addition, *Maackia*

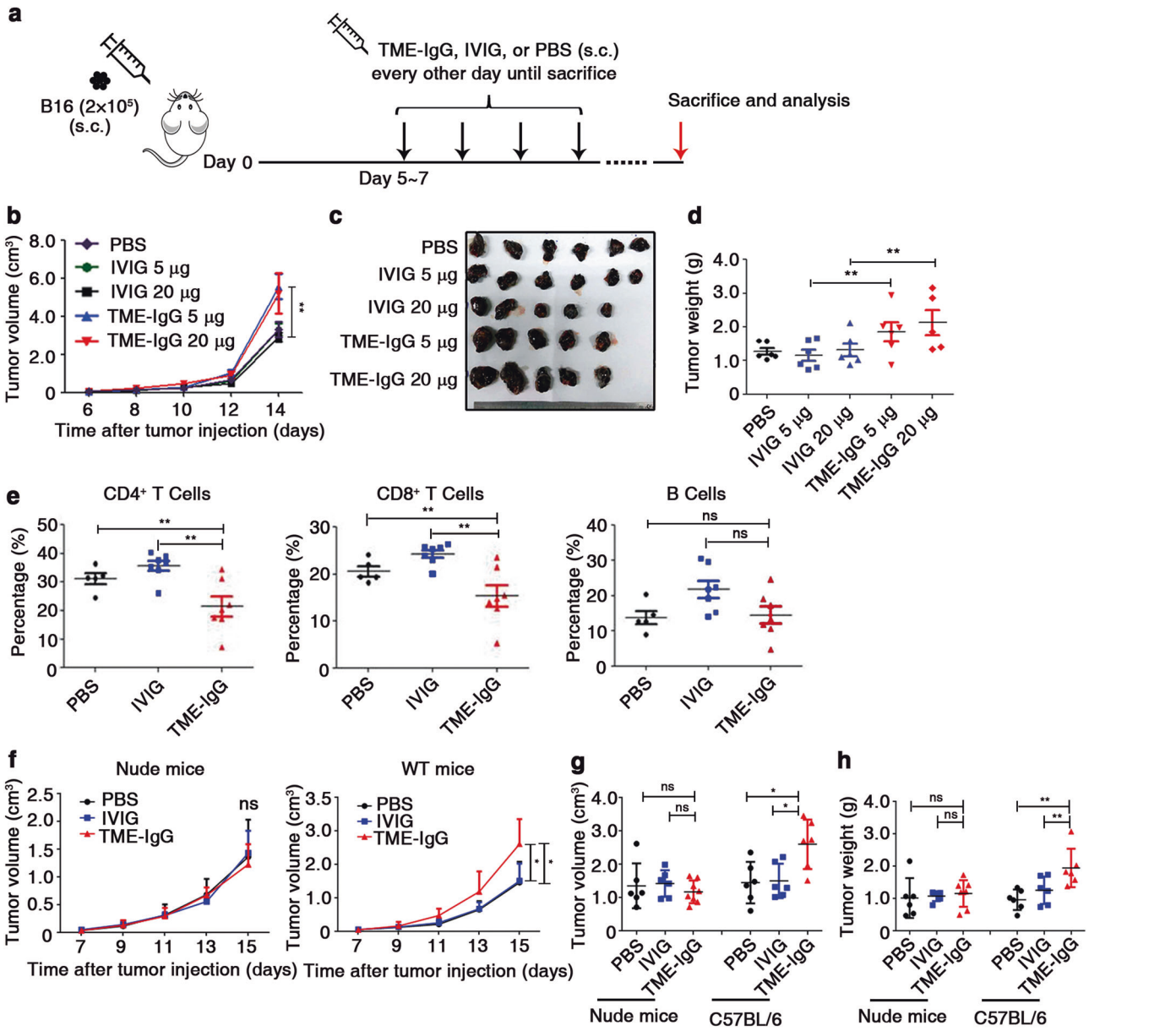

Fig. 2 TME-IgG promotes tumor growth by decreasing the proportions of both $CD4^+$ and $CD8^+$ T cells. **a** Establishment of mouse models used in (**b**–**h**). **b** On the 6th day after subcutaneous (s.c.) injection of B16 cells, 5 μg or 20 μg TME-IgG dissolved in 100 μl PBS ($n = 5$ per group), IVIG ($n = 6$ (5 μg), and $n = 5$ (20 μg)), or 100 μl PBS ($n = 6$ per group) was injected subcutaneously into the peritumoral area, and the tumor volume of each group was measured. Images of the tumors were taken (**c**), and tumor weights (**d**) were measured on day 14 in mice, as in (**b**). **e** Proportions of T and B lymphocytes in the draining lymph nodes (DLNs) of each group (TME-IgG, $n = 7$ (four samples from the 20-μg group and three samples from the 5-μg group); IVIG, $n = 7$ (four samples from the 20-μg group and three samples from the 5-μg group); and PBS, $n = 5$). Tumor growth curves of nude mice (TME-IgG, $n = 8$; IVIG and PBS, $n = 6$) or wild-type C57BL/6 mice ($n = 6$ for each group) treated with 20 μg TME-IgG or IVIG dissolved in PBS or the same volume of PBS (control) are shown in (**f**). Tumor volume (**g**) and weight (**h**) were measured on the 17th day after B16 implantation. Each symbol represents an individual tumor sample; small horizontal lines indicate the mean (± s.e.m. in **b**, **d**, and **e**; ± s.d. in **f**, **g**, and **h**). ns, not significant ($P \geq 0.05$); $^{*}P \leq 0.05$; and $^{**}P \leq 0.01$ (one-way analysis of variance (ANOVA) followed by Tukey's multiple-comparisons test (**b**, **d**, **e**–**h**)). Data are from one experiment that was representative of four (**b**–**e**) independent experiments with similar results. Also see Supplementary Fig. S2.

amurensis lectin II (MAL II), a lectin specific for α2,3 sialic acids, was also used to determine the sialylation state of SIA-CIgG. We used α2,3 neuraminidase to remove α2,3 terminal sialic acids on SIA-CIgG, and the result showed that the signal for RP215 remained unchanged (Supplementary Fig. S3b). Next, we investigated whether the inhibitory effect of SIA-CIgG on T cells was sialylation dependent. Utilizing an SNA affinity column, we first enriched sialylated IgG from total TME-IgG (Fig. 4b) or used neuraminidase to remove terminal sialic acids from SIA-CIgG (Fig. 4c). The Cancer-IgG samples in which sialic acids had been enriched or removed were then used to treat sorted T cells that were stimulated with anti-CD3 and anti-CD28 mAbs. The results showed that the enriched SIA-CIgG fractions, but not the nonbinding fractions of IgG, displayed strong inhibitory effects on $CD4^+$ and $CD8^+$ T cells (Fig. 4d). In contrast, the inhibitory effect of SIA-CIgG on T cells, especially $CD8^+$ T cells, was significantly reduced after the sialic acids were removed (Fig. 4e).

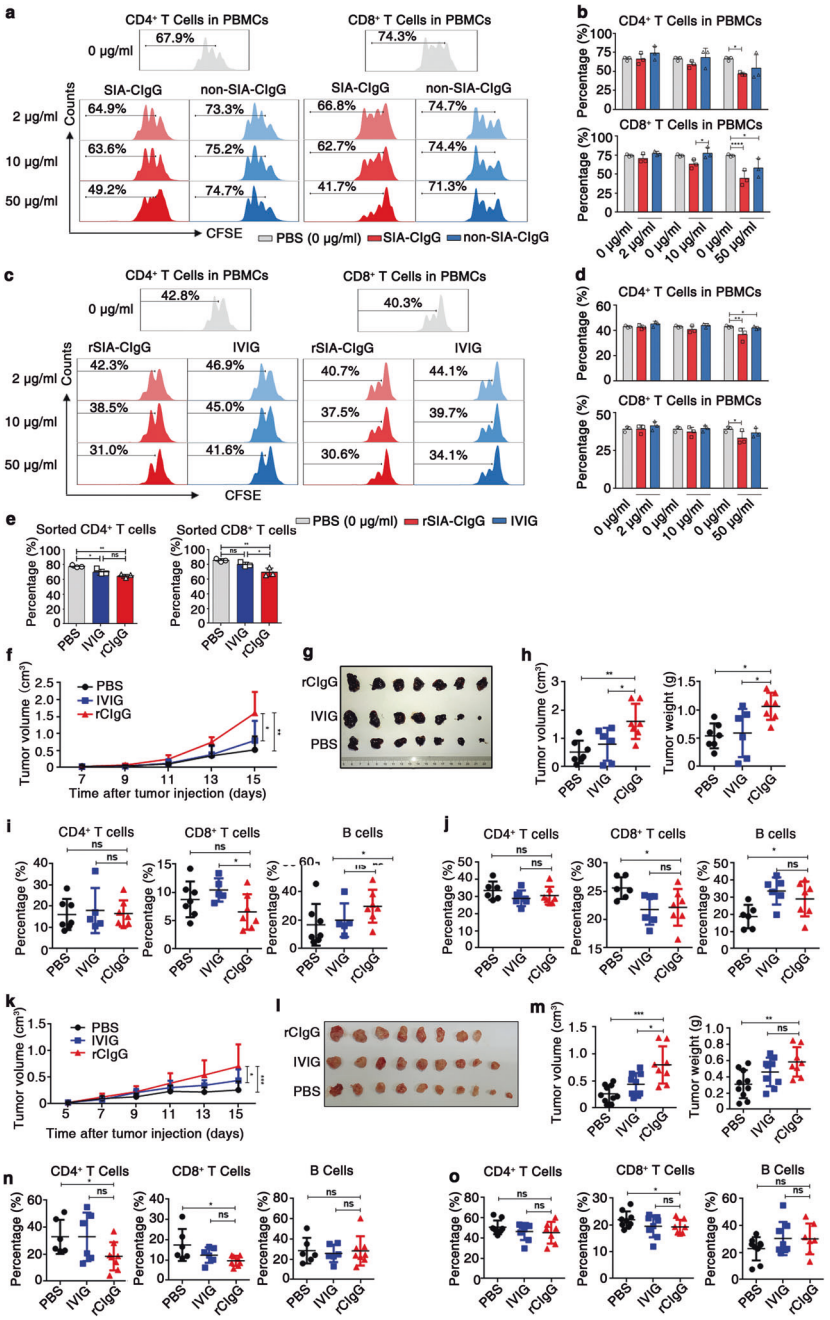

Fig. 3 Inhibition of proliferation and promotion of tumor immune escape mediated by Cancer-IgG. **a** SIA-CIgG was purified from TME-IgG by an RP215 affinity column, then PBS, SIA-CIgG, or non-SIA-CIgG (the fraction of TME-IgG that did not bind to the RP215 affinity column) was added to peripheral blood mononuclear cells (PBMCs) that were activated as described in Fig. 1f. The proliferation of CFSE-labeled $CD4^+$ and $CD8^+$ T cells was measured after 72 h. The doses of SIA-CIgG or non-SIA-CIgG were 2 μg/ml, 10 μg/ml, and 50 μg/ml. **b** Proportions and statistical significance of proliferating $CD4^+$ and $CD8^+$ T cells among all PBMCs treated by SIA-CIgG or non-SIA-CIgG as described in (**a**) ($n = 3$ each group), as evaluated by flow cytometry. **c** Proliferation of activated CFSE-labeled $CD4^+$ and $CD8^+$ T cells treated with rSIA-CIgG or IVIG in the PBMC culture system. The doses of rSIA-CIgG or IVIG were 2 μg/ml, 10 μg/ml, and 50 μg/ml. **d** Proportions and statistical significance of proliferating $CD4^+$ and $CD8^+$ T cells among all PBMCs treated with rSIA-CIgG or IVIG as described in (**c**) ($n = 3$ each group), as determined by flow cytometry. **e** Proportions of proliferating $CD4^+$ and $CD8^+$ T cells sorted by flow cytometry and treated with rCIgG (rSIA-CIgG) or IVIG at a dose of 50 μg/ml ($n = 3$ each group). Small horizontal lines (**b**, **d**, and **e**) indicate the mean (± s.d.). ns, not significant ($P \geq 0.05$); $^{*}P \leq 0.05$; $^{**}P \leq 0.01$; and $^{****}P \leq 0.0001$ (two-tailed Student's *t* test for unpaired data). The protumor effect of subcutaneously injected rCIgG (20 μg, $n = 7$), IVIG (20 μg, $n = 6$), or PBS ($n = 7$) in C57BL/6 mice was measured by evaluating tumor growth (**f**), tumor images (**g**), and tumor volume and weight (**h**) on the 15th day after B16 injection. The proportions of lymphocytes in tumor tissue (**i**) and DLNs (**j**) were measured by flow cytometry. Tumor growth curves (**k**) of rCIgG- (20 μg, $n = 8$), IVIG- (20 μg, $n = 9$), and PBS-treated ($n = 10$) BALB/c mice, tumor images (**l**), and tumor volume and weight (**m**) were determined on the 15th day after injection of EMT-6 cells. **n** The proportions of lymphocytes in tumor tissue. **o** The proportions of lymphocytes in DLNs (rCIgG, $n = 8$; IVIG and PBS, $n = 6$). Each symbol represents an individual tumor sample; small horizontal lines indicate the mean (± s.d.). ns, not significant ($P \geq 0.05$); $^{*}P \leq 0.05$; $^{**}P \leq 0.01$; and $^{***}P \leq 0.001$ (one-way ANOVA followed by Tukey's multiple-comparisons test). Data are from one experiment that was representative of three (**a**) or six (**c**) independent experiments with similar results. Also see Supplementary Fig. S3a.

To determine if the protumor effect of SIA-CIgG depended on its sialylation, we used neuraminidase to remove sialic acids from SIA-CIgG and treated B16 model mice as described above. We found that after removing the sialic acids, the protumor effect of SIA-CIgG was significantly reduced (Fig. 4f, g). Correspondingly, the populations of effector $CD4^+$ and $CD8^+$ T cells in the DLNs were evidently enhanced (Fig. 4h). We also removed sialic acids from rSIA-CIgG and treated EMT-6 model mice in vivo with the treated rSIA-CIgG. Similarly, the protumor effect of rSIA-CIgG was significantly reduced (Supplementary Fig. S3c–e), and the proportion of effector $CD8^+$ T cells in the tumor tissue was enhanced (Supplementary Fig. S3f). To exclude the direct inhibitory effects of neuraminidase on EMT-6 cancer cells, we used neuraminidase to treat EMT-6 model mice in vivo, and the results showed that there was no significant difference in the in vivo protumor effect between neuraminidase and a PBS control (Supplementary Fig. S3g–i). Since the monoclonal antibody RP215 only recognizes the sialylated epitope of Cancer-IgG,[14] we used RP215 to bind the sialylated epitope of SIA-CIgG before SIA-CIgG was used to treat B16 model mice in vivo. As expected, RP215 treatment significantly decreased the protumor effect of SIA-CIgG and reversed the reductions in $CD4^+$ and $CD8^+$ T-cell frequencies in the DLNs (Fig. 4i, j). Collectively, these results demonstrate that the inhibitory effect of SIA-CIgG on effector T cells is dependent on SIA-CIgG sialylation.

Fab fragments of SIA-CIgG containing the CH1 domain that are recognized by RP215 display a strong inhibitory effect on T-cell proliferation

To further explore whether the inhibitory effect of SIA-CIgG is dependent on the CH1 domain recognized by RP215, papain was used for digestion to obtain Fab and Fc fragments (Fig. 5a). As is shown, RP215 only recognized Fab fragments and undigested IgG, not Fc fragments (Fig. 5b, c).

Next, we addressed whether the RP215-recognized Fab fragments of SIA-CIgG containing the CH1 domain display a strong inhibitory effect on T-cell proliferation. Fab fragments were used to treat sorted human T cells stimulated with anti-CD3 and anti-CD28 mAbs in vitro, and Fc fragments (containing some undigested SIA-CIgG) were used as controls. Although both the Fab fragments and the control (Fc fragments and undigested SIA-CIgG) displayed strong inhibitory effects on $CD4^+$ and $CD8^+$ T cells that were dose dependent, the Fab fragments showed stronger inhibitory effects than the Fc fragments (Fig. 5d, e).

Next, Fab fragments were used to treat EMT-6 model mice, as described above. As expected, we found that Fab fragments but not controls, including PBS and Fc fragments mixed with undigested SIA-CIgG, showed a significant protumor effect (Fig. 5f–h). Moreover, effector $CD4^+$ and $CD8^+$ T-cell infiltration into tumor tissue was decreased (Fig. 5i). Thus, these data demonstrate that RP215-recognized Fab fragments of SIA-CIgG containing the CH1 domain have a strong inhibitory effect on T-cell proliferation.

Siglecs mediate the suppression of T-cell proliferation induced by SIA-CIgG

As shown above, SIA-CIgG directly suppressed T-cell proliferation. Hence, we hypothesized that SIA-CIgG binds to some suppressive sialic acid receptors on the surface of T cells. We first determined whether SIA-CIgG directly binds to the T-cell surface of cells in either the resting or activated state. The results indicated that SIA-CIgG could bind to resting $CD8^+$ T cells, but hardly bound to resting $CD4^+$ T cells. However, after the T cells were stimulated by phytohemagglutinin (PHA) or anti-CD3 and anti-CD28 mAbs, the binding of SIA-CIgG to $CD4^+$ or $CD8^+$ T cells significantly increased (Fig. 6a). Correspondingly, after mouse T cells were stimulated by anti-CD3 and anti-CD28 mAbs, the binding of human SIA-CIgG to the mouse $CD4^+$ or $CD8^+$ T cells also increased (Fig. 6b). These results suggested that there were some unidentified receptors for SIA-CIgG on activated $CD4^+$ and $CD8^+$ T cells.

Siglecs have been reported to be sialic acid-binding receptors, and the Siglec family includes 15 members in humans and 9 members in mice.[42] Siglecs can transmit either inhibitory (human: Siglec-2, Siglec-3, Siglec-5, Siglec-6, Siglec-7, Siglec-8, Siglec-9, Siglec-10, and Siglec-11; mouse: Siglec-2, Siglec-3, Siglec-E, Siglec-F, and Siglec-G) or activating (human: Siglec-14, Siglec-15, and Siglec-16; mouse: Siglec-H and Siglec-15) signals depending on the presence of immunoreceptor tyrosine-based inhibitory motifs (ITIMs) or immunoreceptor tyrosine-based activation motifs (ITAMs), respectively, in the cytosolic region. Notably, most Siglecs provide an inhibitory signal to immune cells.[2328,29,43] Because the inhibitory effect of SIA-CIgG is dependent on sialic acid modification, we tried to identify inhibitory Siglecs that can be expressed on T cells. We first used the ImmuSort website (http://immusort.bjmu.edu.cn)[44] to analyze the gene expression of all Siglec members with ITIMs from 433 datasets containing 10,422 human samples in the GEO database and found that the genes encoding Siglec-6, Siglec-7, and Siglec-10 were expressed at significant levels in human $CD4^+$ and $CD8^+$ T cells (Supplementary Fig. S4a). In addition, from 455 datasets containing 3929 mouse samples, we found that the mouse homologs of the human Siglec-3 and Siglec-10 genes, named the Siglec-3 (CD33) and Siglec-G (Siglec-10) genes, were expressed at significant levels in mouse $CD4^+$ and $CD8^+$ T cells (Supplementary Fig. S4b). Next, we determined whether Siglec transcripts are expressed in activated or resting $CD4^+$ or $CD8^+$ T cells sorted from humans or mice. We found that human Siglecs, such as *Siglec-3*, *Siglec-6*, *Siglec-10, Siglec-15*, and *Siglec-16*, were expressed in both resting and activated $CD4^+$ and $CD8^+$ T cells. However, *Siglec-7* was only detected in activated $CD4^+$ and $CD8^+$ T cells. Mouse *Siglec-E* and *Siglec-G* were expressed in both resting and activated $CD4^+$ and $CD8^+$ T cells. However, mouse *Siglec-3* was only detected in activated $CD4^+$ and $CD8^+$ T cells (Fig. 6c). The transcripts of other human Siglecs were not detected in T cells (Supplementary Fig. S5a). Subsequently, Siglec-7 and Siglec-10 expression was found on both $CD4^+$ and $CD8^+$ T cells by flow cytometry (Supplementary Fig. S5b). Moreover, mouse Siglec-G was determined to be expressed on both $CD4^+$ and $CD8^+$ T cells (Supplementary Fig. S5c). Importantly, neutralizing antibodies for either Siglec-7 or Siglec-10 significantly blocked the SIA-CIgG-mediated inhibition of $CD4^+$ and $CD8^+$ T-cell proliferation (Fig. 6d).

We next investigated whether Siglecs interact with SIA-CIgG by overexpressing human Siglec-10 in the lung cancer cell line NCI-H520. We found that endogenous SIA-CIgG interacted with exogenous Siglec-10 by coimmunoprecipitation (Co-IP) (Fig. 6e, f). Correspondingly, we coexpressed one of three mouse inhibitory Siglecs (Siglec-3, Siglec-E, and Siglec-G) and human SIA-CIgG in the cell line 293T, and found that human GFP-SIA-CIgG interacted with exogenous Myc-Siglec-G and Myc-Siglec-E by Co-IP (Fig. 6g, h; Supplementary Fig. S5d, e). In contrast, exogenous His-Siglec-3 (CD33) did not interact with GFP-SIA-CIgG (Supplementary Fig. S5f).

Siglecs are highly expressed in effector T cells from patients with cancer but not those from healthy donors

Since SIA-CIgG inhibited T-cell proliferation by interacting with Siglecs, we examined whether Siglecs with ITIMs are expressed on effector T cells in the peripheral blood or TME of cancer patients. We first analyzed the transcripts of Siglec family members in tumor-specific $CD8^+$ T cells from patients with melanoma or head and neck cancer, $CD8^+$ T cells in the TME of patients with lung cancer and $CD4^+$ T cells in the peripheral blood of patients with breast cancer in microarray or RNA-Seq datasets from the GEO database. The results for 18 melanoma patients (GSE24536) revealed that there was a significant increase in *Siglec-10* expression in tumor-specific $CD8^+$ T cells compared to naive

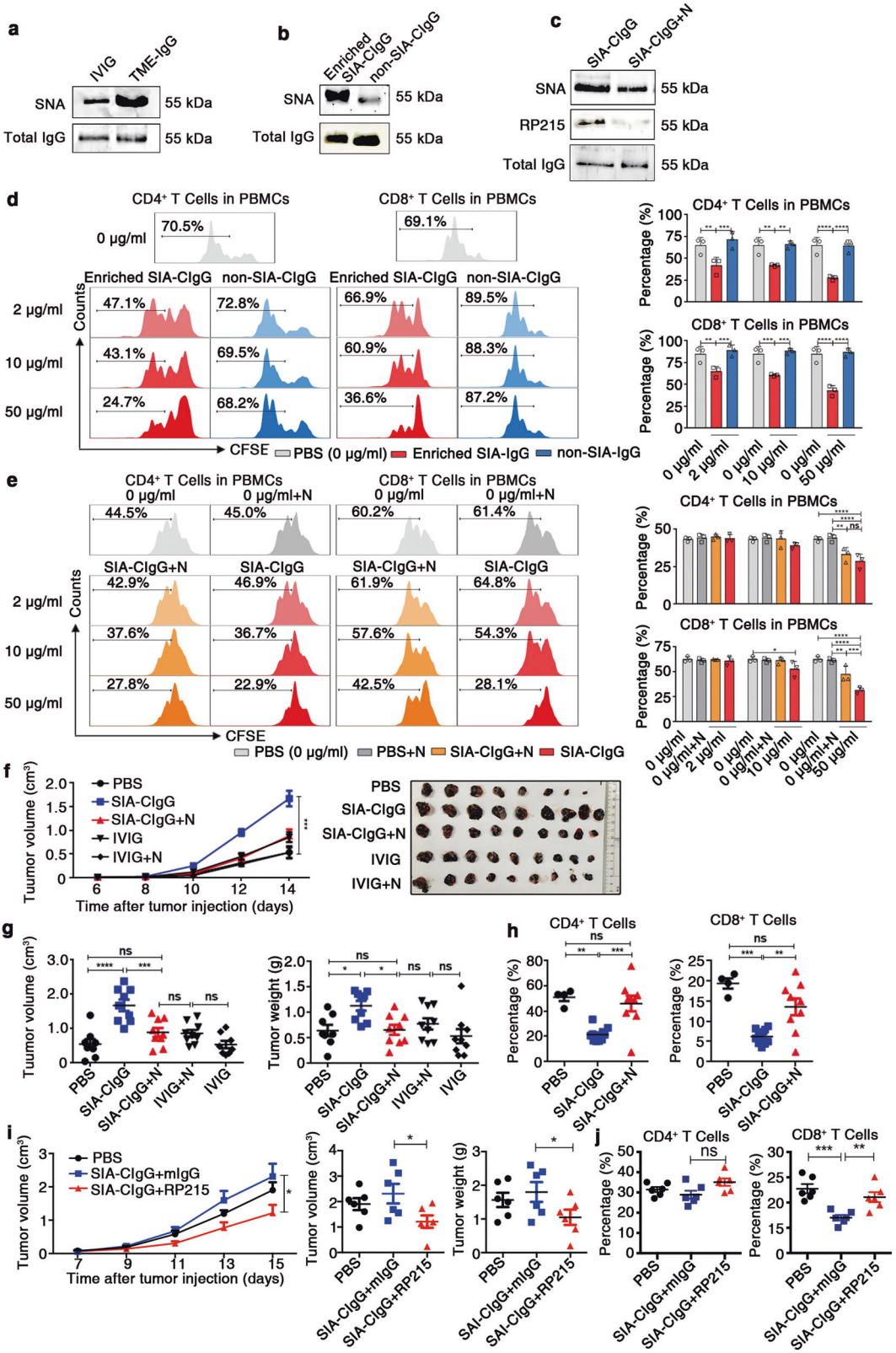

CD8$^+$ T cells (Supplementary Fig. S6a). Similarly, compared with CD8$^+$ T cells that infiltrated adjacent tissues, CD8$^+$ T cells in the non-small cell lung carcinoma (NSCLC; adenocarcinoma or squamous carcinoma) TME (GSE90728) expressed higher levels of *Siglec-10* (Supplementary Fig. S6b). *Siglec-7* and *Siglec-10* were also overexpressed in tumor-specific CD8$^+$ T cells compared with nonspecific CD8$^+$ T cells in head and neck cancer (squamous cell carcinoma) (GSE114944) (Supplementary Fig. S6c). Similarly, the expression of *Siglec-3*, *Siglec-7*, *Siglec-9*, and *Siglec-10* was also higher in the peripheral blood CD4$^+$ T cells of patients with breast cancer (invasive ductal carcinoma) (GSE36765) than in those of healthy donors, but the difference was not significant

Fig. 4 Inhibitory effect of Cancer-IgG on T cells is sialylation dependent. **a** Comparison of the sialylation state between TME-IgG and IVIG. The sialylation state was identified by SNA lectin blotting (upper panel), and total IgG was estimated with a commercial anti-IgG antibody by western blotting (lower panel). **b** SIA-CIgG was enriched by an SNA affinity column. The sialylation state of SIA-CIgG and nonsialylated Cancer-IgG (the nonbinding fractions) was determined by SNA lectin blotting (upper panel) and western blotting (lower panel). **c** Sialic acid residues in SIA-CIgG were digested with neuraminidase, and SIA-CIgG was identified by SNA lectin, RP215, or a commercial anti-IgG antibody. N, neuraminidase. **d** Proliferation (left) and proportions (right) of CFSE-labeled $CD4^+$ and $CD8^+$ T cells treated with Enriched SIA-CIgG or non-SIA-CIgG. The doses of Enriched SIA-CIgG and non-SIA-CIgG were 2 μg/ml, 10 μg/ml, and 50 μg/ml. **e** Proliferation (left) and proportions (right) of CFSE-labeled $CD4^+$ and $CD8^+$ T cells treated with PBS, neuraminidase, SIA-CIgG, or sialic acid-removed Cancer-IgG. The doses of SIA-CIgG or sialic acid-removed Cancer-IgG were 2 μg/ml, 10 μg/ml, and 50 μg/ml. Small horizontal lines (**d** and **e** right) indicate the mean (± s.d.). ns, not significant ($P \geq 0.05$); $^{*}P \leq 0.05$; $^{**}P \leq 0.01$; $^{***}P \leq 0.001$; and $^{****}P \leq 0.0001$ (two-tailed Student's *t* test for unpaired data). Tumor growth curves, tumor images (**f**), and tumor volume and weight (**g**) were determined on the 14th day after injection of B16 cells into C57BL/6 mice (PBS, $n = 8$; SIA-CIgG, SIA-CIgG digested with neuraminidase, IVIG, and IVIG digested with neuraminidase, $n = 9$ per group). Key to (**f**). **h** Proportions of lymphocytes in the DLNs of mice treated with SIA-CIgG ($n = 9$), SIA-CIgG digested with neuraminidase ($n = 9$) or PBS ($n = 4$). Key to (**f**). **i** Tumor growth curves and tumor volume and weight were determined on the 15th day after injection of B16 cells into C57BL/6 mice and treatment with 5 μg SIA-CIgG and 5 μg RP215 (or mouse IgG or PBS) ($n = 6$). **j** Proportions of T cells in DLNs. Each symbol represents an individual tumor sample; small horizontal lines indicate the mean (± s.e.m.). ns, not significant ($P \geq 0.05$); $^{*}P \leq 0.05$; $^{**}P \leq 0.01$; $^{***}P \leq 0.001$; and $^{****}P \leq 0.0001$ (one-way ANOVA followed by Tukey's multiple-comparisons test). Data are from one experiment that was representative of three (**a**–**c**) or six (**d**, **e**) independent experiments with similar results. Also see Fig. S3c–i.

(Supplementary Fig. S6d). In addition, Kwok-Kin Wong's group showed that treating lung tumor model mice with the CDK4/6 inhibitor G1T28 enhanced T-cell activity, contributing to antitumor effects in vivo.[45] By analyzing mouse RNA-Seq datasets in the GEO database (GSE89477) to examine the expression of suppressive Siglecs in individual tumor-infiltrating T cells in mouse lung cancer, we found significant increases in *Siglec-3* and *Siglec-G* expression in activated T cells (treated with G1T28) compared with control T cells (Supplementary Fig. S7e).

Subsequently, we analyzed the expression of Siglec-3, Siglec-6, Siglec-7, and Siglec-10 on effector T cells in the peripheral blood of 13 patients with head and neck cancer, 19 patients with lung cancer, and 26 control healthy donors by flow cytometry (Siglec-9: 19 patients with lung cancer and 37 healthy donors). We found that Siglec-3, Siglec-6, Siglec-7, Siglec-9, and Siglec-10 levels in the $CD4^+$ T cells, and Siglec-3 and Siglec-6 levels in the $CD8^+$ T cells of the patients with lung cancer were significantly elevated compared to those in the corresponding cells of the healthy donors. In addition, the expression of Siglec-6 in $CD4^+$ T cells and that of Siglec-3, Siglec-6, Siglec-7, and Siglec-10 in $CD8^+$ T cells were also significantly higher in the patients with head and neck cancer (Fig. 7a) than in the healthy donors. Correspondingly, we isolated tumor-infiltrating T cells from EMT-6 tumor model mice that were treated with rSIA-CIgG with or without sialic acid and analyzed the expression of Siglec-3, Siglec-E, and Siglec-G on the T cells by flow cytometry. The results showed that the Siglec-G and Siglec-E expression in the T cells treated with rSIA-CIgG was significantly elevated compared with that in the T cells from control mice (Fig. 7b). These results provide indications that Siglecs, especially Siglec-10, may serve as potential immune checkpoint molecules that facilitate tumor immune escape by interacting with SIA-CIgG.

In addition, we also compared the expression levels of Siglecs with those of two well-known checkpoint molecules, *PD-1* and *CTLA-4*, in the $CD4^+$ and $CD8^+$ T cells of cancer patients, as described above. We found similar expression levels between most Siglecs and PD-1 or CTLA-4 in the $CD4^+$ and $CD8^+$ T cells of head and neck cancer patients (Supplementary Fig. S6f, g); however, no or little coexpression was observed between Siglecs and either *PD-1* or *CTLA-4* in the $CD4^+$ and $CD8^+$ T cells analyzed in this study (Supplementary Fig. S6h). However, *Siglec-6* and *Siglec-7* showed significant coexpression with *CTLA-4* in the $CD8^+$ T cells of five patients with head and neck cancer (Fig. 7c).

DISCUSSION

To date, IgG deposits in the TME have been believed to be produced by B cells and to generally have antitumor activity. However, in this study, we found that IgG deposits in the TME contained a large portion of cancer-derived IgG. Importantly, we found for the first time that Cancer-IgG could be involved in tumor immune evasion by directly inhibiting proliferation and reducing the proportions of effector $CD4^+$ and $CD8^+$ T cells. Mechanistic research showed that Cancer-IgG could bind to the sialic acid receptors called Siglecs expressed on effector T cells via a unique sialylation of the CH1 domain and could promote the maintenance of the immunosuppressive TME.

Historically, only B cells were believed to produce Igs, but a growing body of evidence has shown that most non-B cells can also express Igs and that cancer cells usually overexpress IgG.[4–8,11,34,46,47] However, for a long time, we could not distinguish Cancer-IgG from B-IgG with the commercial anti-IgG antibody that we previously used. Recently, using mAb-RP215, which mainly recognizes Cancer-IgG but not B-IgG, we identified a unique sialic acid modification on Cancer-IgG that occurs as an N-glycosylation-related sialylation modification at the Asn162 site but not the classic Asn297 site.[14] Therefore, the unique sialylation modification recognized by RP215 can distinguish Cancer-IgG from B-IgG.

Cancer-IgG has been shown to promote tumorigenesis and metastasis via various mechanisms that are different from those of IgG antibodies.[8,10,11,48] Cancer-IgG overexpression is indicative of a high metastatic ability and poor prognosis;[11,37,38,49] however, the protumor effect of Cancer-IgG is not fully understood. Recently, using RP215, we found that SIA-CIgG, which carries a unique sialic acid modification, was overexpressed in many epithelial cancer cells, especially in the corresponding cancer stem cells. Importantly, SIA-CIgG maintains the biological behaviors of cancer stem cells, such as self-renewal, drug resistance and metastasis.[35] Mechanistic research has indicated that Cancer-IgG can activate the FAK pathway by binding to integrin a6β4 on cancer stem cells.[14] However, whether SIA-CIgG is involved in tumor immune escape remains unclear.

Given that the sialylated IgM and sialylated IgG in IVIG have immunomodulatory effects on effector T cells,[17] we hypothesized that SIA-CIgG may be involved in tumor immune escape by inhibiting T-cell activity. In this study, we found that unlike the sialylated IgG in IVIG, which was previously reported to indirectly inhibit T-cell activity by directly suppressing myeloid cells, surprisingly, SIA-CIgG could directly inhibit the proliferation of effector T cells, especially $CD8^+$ T cells, in vitro. More importantly, SIA-CIgG could significantly promote tumor progression and reduce effector T-cell frequencies in vivo. However, in T-cell-deficient mice, SIA-CIgG did not have a protumor effect. Notably, the protumor effect of SIA-CIgG was T-cell dependent. Moreover, unlike the sialylated IgG in IVIG, for which the inhibitory effect on myeloid cells depends on the classic Asn297 sialylation epitope in the Fc region, SIA-CIgG mediated its inhibitory effect on effector

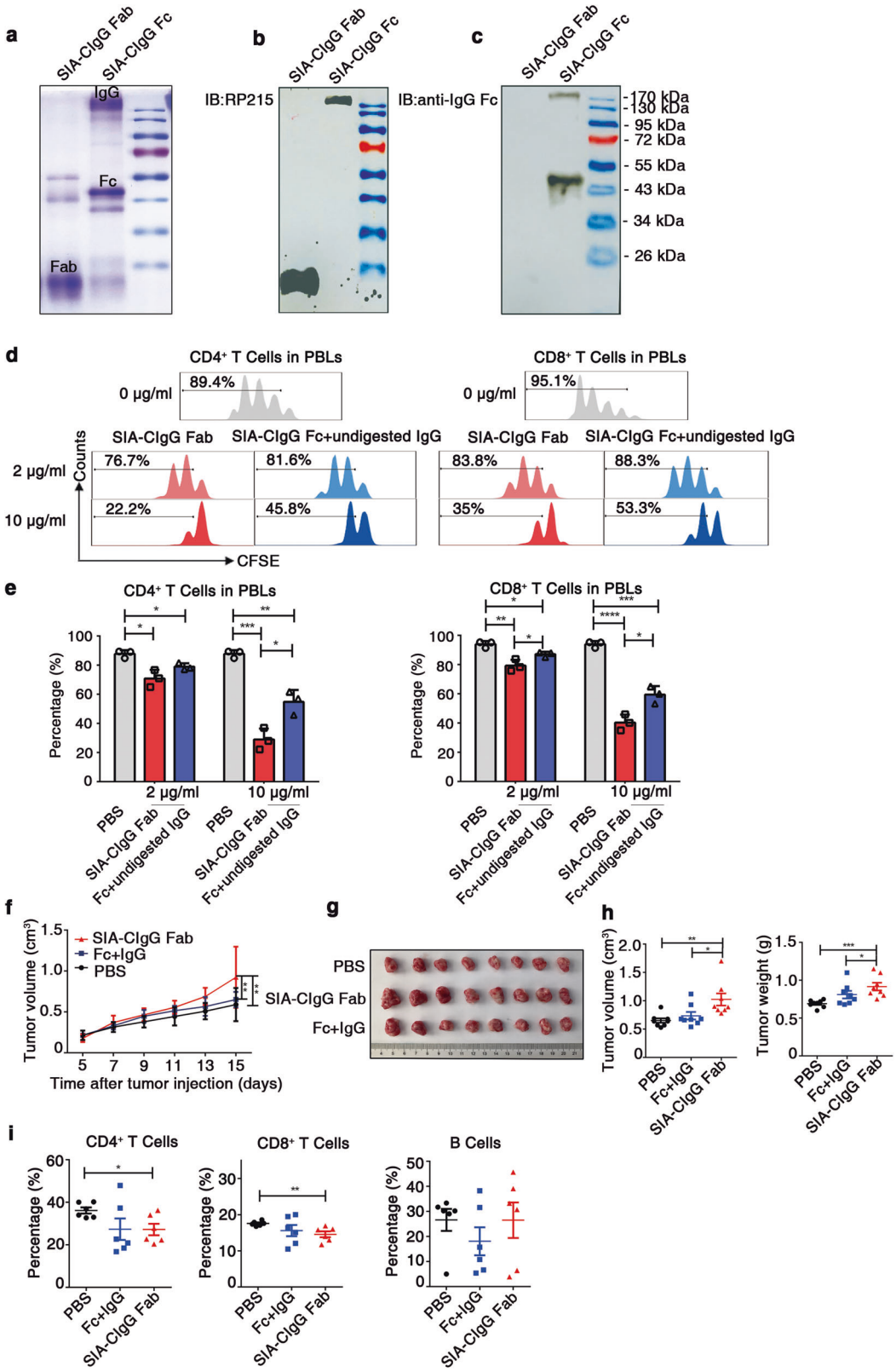

T cells via the distinctive Asn162 sialylation epitope, which is specifically recognized by RP215.[14]

Increased levels of sialic acid are pervasive in cancer, and a growing body of evidence demonstrates how hypersialylation is advantageous to cancer cells, particularly from the perspective of modulating immune responses. Sialic acid-binding receptors, such as Siglecs, are well positioned to be exploited by cancer hypersialylation. Mounting evidence also shows that Siglecs modulate key immune cell types in the TME.[50] Siglecs have been frequently found to be expressed on innate immune cells, such as

Fig. 5 Fab fragments of SIA-CIgG containing the CH1 domain that are recognized by RP215 display a strong inhibitory effect on T-cell proliferation. **a** Coomassie light blue staining of SIA-CIgG Fab and SIA-CIgG Fc fragments digested by papain. The sialylation site was identified with RP215 (**b**) and a commercial anti-human-IgG Fc antibody (**c**) by western blotting. **d** SIA-CIgG Fab and SIA-CIgG Fc + undigested IgG fragments were digested by papain. Then, PBS, the SIA-CIgG Fab fragments or the SIA-CIgG Fc + undigested IgG fragments were added to peripheral blood lymphocytes (PBLs) that were activated as described in Fig. 1f. The proliferation of CFSE-labeled $CD4^+$ and $CD8^+$ T cells was measured after 72 h. The doses of SIA-CIgG Fab fragments or SIA-CIgG Fc + undigested IgG fragments were 0 μg/ml, 2 μg/ml, and 10 μg/ml. **e** Proportions and statistical significance of proliferating $CD4^+$ and $CD8^+$ T cells among all PBLs treated with PBS, SIA-CIgG Fab fragments or SIA-CIgG Fc + undigested IgG fragments (Fc + undigested IgG) as described in (**d**) ($n = 3$ each group), as determined by flow cytometry. Small horizontal lines (**e**) indicate the mean (± s.d.). $^*P \le 0.05$, $^{**}P \le 0.01$, $^{***}P \le 0.001$, and $^{****}P \le 0.0001$ (two-tailed Student's *t* test for unpaired data). Tumor growth curves (**f**), tumor images (**g**), and tumor volume and weight (**h**) were determined on the 15th day after injection of EMT-6 cells into BALB/c mice (PBS, $n = 8$; SIA-CIgG Fab, 20 μg, $n = 8$; and SIA-CIgG Fc + undigested IgG, 20 μg, $n = 8$). **i** Proportions of lymphocytes in the tumors of mice treated with PBS ($n = 8$), SIA-CIgG Fab fragments ($n = 8$), or SIA-CIgG Fc + undigested IgG fragments (Fc + IgG) ($n = 8$). Each symbol represents an individual tumor sample; small horizontal lines indicate the mean (± s.e.m.). $^*P \le 0.05$, $^{**}P \le 0.01$, $^{***}P \le 0.001$, and $^{****}P \le 0.0001$ (one-way ANOVA followed by Tukey's multiple-comparisons test). Data are from one experiment that was representative of three (**a**–**d**) or two (**f**–**i**) independent experiments with similar results.

tumor-associated neutrophils, tumor-associated macrophages,[31,50,51] NK cells, dendritic cells, and B cells.[43] However, the results for whether Siglecs are expressed on T cells have not been consistent; in fact, as early as 1999, Siglec-7 was found on a minor subset of $CD8^+$ T cells,[26] and then siglec-9 was observed on minor subsets of $CD8^+$ and $CD4^+$ T cells.[27] In recent years, a growing body of evidence has proven that several Siglecs, such as Siglec-3, Siglec-7, Siglec-9, and Siglec-10, are found on normal and tumor-infiltrating T cells[25–32], and that the Siglecs expressed on T cells can suppress T-cell activation and proliferation.[29,30,32] In particular, Siglec-9 expression has been found to be upregulated on tumor-infiltrating T cells from patients with NSCLC, colorectal cancer, or ovarian cancer. Siglec-9 was identified as a potential target for improving T-cell activation by immunotherapy.[30] Therefore, we hypothesized that SIA-CIgG can also bind T cells via Siglecs.

We first observed that SIA-CIgG could bind to the cell surface of $CD4^+$ and $CD8^+$ T cells, by RT-PCR and flow cytometry, found that Siglec-3, Siglec-6, Siglec-7, and Siglec-10 were expressed on resting and activated $CD8^+$ T cells and activated $CD4^+$ T cells. Furthermore, neutralizing antibodies against either Siglec-7 or Siglec-10 significantly blocked the SIA-CIgG-mediated inhibition of $CD4^+$ and $CD8^+$ T-cell proliferation. Importantly, we found that SIA-CIgG interacted with Siglec-10 by Co-IP. It is important to note that like mouse TME-IgG, human SIA-CIgG has an immunosuppressive effect on mouse T-cell proliferation that involves binding to mouse Siglecs. These results suggest that Siglecs on mouse T cells can also recognize human N-acetylneuraminic acid (Neu5Ac, the same sialic acid of mouse Neu5Ac) and mediate immunosuppressive effects.

We then addressed whether T cells in patients with cancer widely express Siglecs. In this study, we first mined the GEO database and found that normal and malignant $CD4^+$ and $CD8^+$ T cells could express Siglec-3, Siglec-6, Siglec-7, and Siglec-10, which contain ITIMs in their cytoplasmic tail.[43] By analyzing microarray or RNA-Seq datasets in the GEO database to examine the expression of Siglec family members, we found a significant increase in *Siglec-10* expression in the tumor-infiltrating $CD8^+$ T cells in patients with NSCLC, and in tumor-specific $CD8^+$ T cells of patients with head and neck cancer or melanoma. Moreover, *Siglec-2, Siglec-3, Siglec-7, Siglec-9,* and *Siglec-10* were also more highly expressed in the peripheral blood $CD4^+$ T cells of patients with breast cancer than in those of healthy donors. Next, we collected peripheral blood from patients with NSCLC or head and neck cancer and healthy donors, which were used as controls, and found that $CD4^+$ and $CD8^+$ T cells could express Siglec-3, Siglec-6, Siglec-7, Siglec-9, and Siglec-10. Importantly, most Siglecs detected in this study were overexpressed on the $CD4^+$ or $CD8^+$ T cells of patients with cancer compared with those of healthy donors, which suggests that Siglecs may serve as potential immune checkpoint molecules and that SIA-CIgG may be a potential ligand of Siglecs.

In addition, we also analyzed whether Siglecs were coexpressed with two well-known immune checkpoint molecules, PD-1 and CTLA-4, in any GEO database or the patients with cancer included in our experiment. We found that Siglecs were not coexpressed with *PD-1* on effector T cells, which suggested that $Siglec^+$ T cells were not exhausted T cells. However, *Siglec-6* and *Siglec-7* were coexpressed with *CTLA-4*, a checkpoint molecule and a marker of the later phase of T-cell activation, in $CD8^+$ T cells from patients with head and neck cancer. Similarly, our results also indicated that Siglecs were expressed at high levels on activated T cells. These results suggest that the expression of Siglecs may be related to T-cell activation.

In summary, we first found that SIA-CIgG, as a potential ligand of Siglecs, could be involved in tumor immune escape via the inhibition of activated effector T cells. In other words, we found a pair of potential checkpoint molecules, SIA-CIgG/Siglec, similar to PD-1/PD-L1. However, unlike PD-1/PD-L1, which mainly suppress activated T cells, SIA-CIgG does not only affect T cells; our results indicate that although effector T cells are the major targets of SIA-CIgG, the NK cell frequency in tumor tissue was significantly decreased, and the frequencies of M2 macrophages and myeloid-derived suppressor cells (MDSCs), two major suppressive populations in the TME, were increased by SIA-CIgG in vivo. Together, these results suggest that SIA-CIgG/Siglec may have broad immunosuppressive activity against different immune cells. However, the detailed mechanism needs to be clarified in further studies.

MATERIALS AND METHODS

Mice

C57BL/6 female mice, BALB/c female mice, female nude mice, NOD SCID mice, and $RAG1^{-/-}$ mice were purchased from Beijing Vital River Laboratory Animal Technology Company and used at 6–8 weeks of age. All mice were housed in a pathogen-free facility at the Peking University Health Science Center (reference number for the ethic offices: LA2019091).

Tissue and peripheral blood samples

Ovarian cancer tissue samples for IgG purification were obtained from Peking University People's Hospital. Human peripheral blood from healthy donors was provided by the Beijing Red Cross Blood Center. Peripheral blood from lung cancer and head and neck cancer patients was provided by the specimen bank of Peking University third hospital. The study was conducted according to an institutional review board-approved protocol.

Cell culture and reagents

The 293T cell line, human lung squamous carcinoma cell line NCI-H520, mouse melanoma cell line B16, and mouse breast cancer

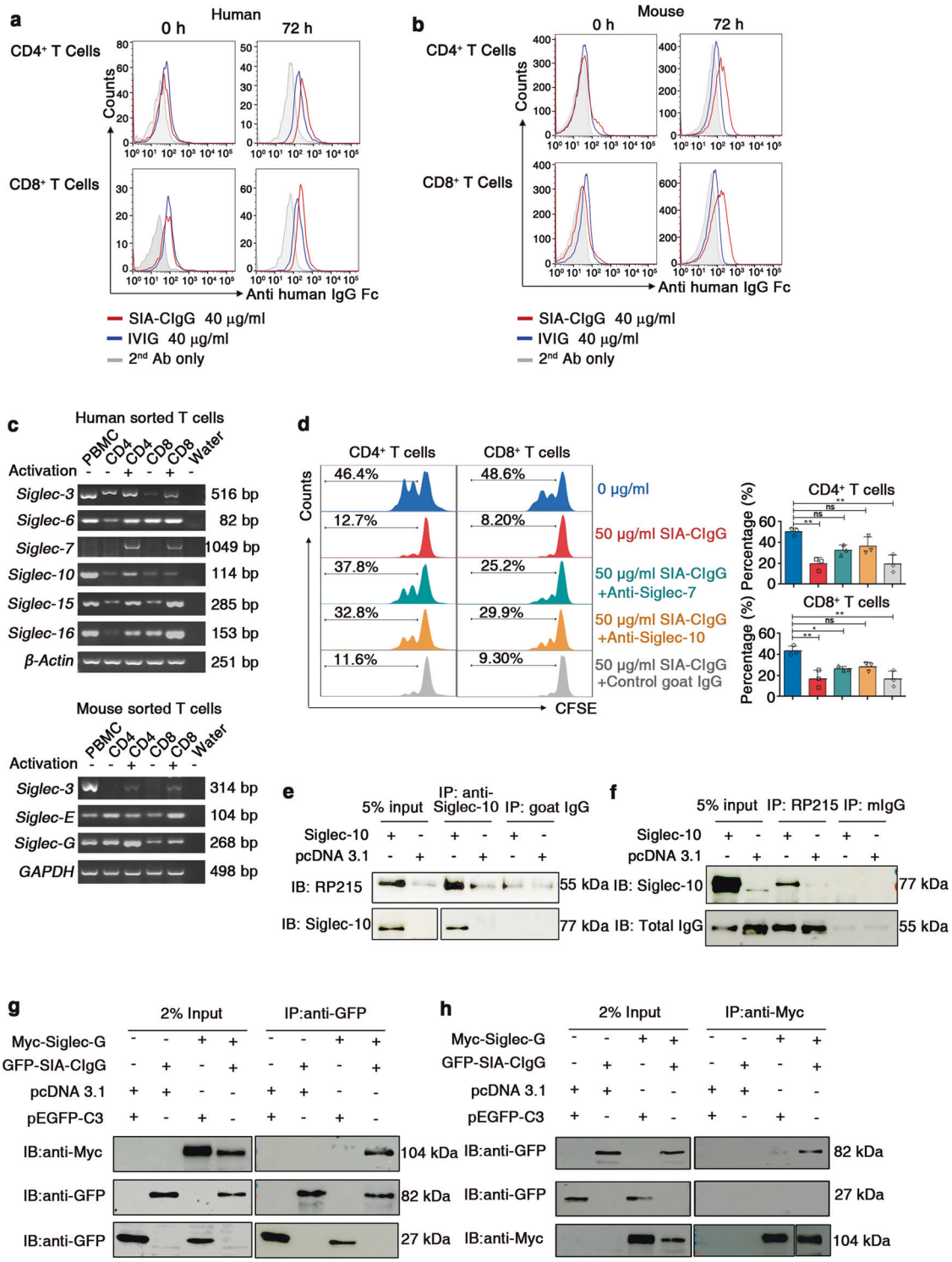

cell line EMT-6 were obtained from the American Type Culture Collection (ATCC), and maintained by the Peking University Center for Human Disease Genomics. Peripheral blood mononuclear cells (PBMCs) were isolated by Ficoll-Hypaque density gradient centrifugation. Peripheral blood lymphocytes (PBLs) were isolated from nonadherent PBMCs after 4 h of culture. T and B cells were sorted from PBMCs using the FACSAria II platform (BD Biosciences). Splenic or lymph node $CD4^+$ T cells and $CD8^+$ T cells from C57BL/6 mice were sorted using the FACSAria II platform (BD Biosciences).

PBMCs, PBLs, sorted T and B cells, and NCI-H520 cells were cultured in RPMI-1640 medium (Thermo Fisher Scientific), 293T, B16 and EMT-6 cells were maintained in Dulbecco's modified Eagle's medium (Thermo Fisher Scientific); all media were supplemented with 10% fetal bovine serum (FBS; HyClone) and a 1% penicillin–streptomycin solution (SV30010, HyClone), and cells were cultured in a humidified atmosphere of 5% CO_2 at 37 °C. All cell lines used in this study were regularly authenticated by morphological observation and tested for the absence of mycoplasma contamination.

Fig. 6 T-cell suppression induced by SIA-CIgG is mediated by Siglecs. **a** Resting human PBMCs activated by 20 μg/ml phytohemagglutinin (PHA) or anti-CD3 and anti-CD28 mAbs for 72 h were incubated with 40 μg/ml SIA-CIgG that was enriched by an RP215 affinity column, 40 μg/ml IVIG or PBS (2nd Ab) for 45 min; washed; and incubated with phycoerythrin (PE)-labeled anti-human IgG. The binding of SIA-CIgG and IVIG was detected by flow cytometry. **b** Resting mouse lymph node-derived $CD4^+$ and $CD8^+$ T cells activated by anti-CD3 and anti-CD28 mAbs for 48 h were incubated with 40 μg/ml SIA-CIgG that was enriched by an RP215 affinity column, 40 μg/ml IVIG or PBS (2nd Ab) for 45 min; washed and incubated with PE-labeled anti-human IgG. The binding of SIA-CIgG and IVIG was detected by flow cytometry. **c** RT-PCR detection of human (upper) and mouse (lower) Siglec gene transcripts in $CD4^+$ and $CD8^+$ T cells sorted by flow cytometry and activated with anti-CD3 and anti-CD28 mAbs or left unstimulated. The PCR mixture without templates was used as a negative control (water), and PBMCs were used as a positive control. **d** Proliferation (left), proportions, and statistical significance (right) of 50 μg/ml SIA-CIgG-treated PBLs blocked with 20 μg/ml goat anti-human Siglec-7 antibody or anti-human Siglec-10 antibody. Nonspecific goat IgG was used as a control. The blocking antibodies were added 2 h prior to the addition of SIA-CIgG. Small horizontal lines (**d** right) indicate the mean (± s.d.). ns, not significant ($P \geq 0.05$); $^{*}P \leq 0.05$; and $^{**}P \leq 0.01$, (two-tailed Student's *t* test for unpaired data). **e**, **f** Interaction between endogenous SIA-CIgG and exogenous Siglec-10 in the human lung cancer cell line NCI-H520, as detected by Co-IP. mIgG, isotype mouse IgG. **g**, **h** Interaction between exogenous Myc-Siglec-G and GFP-SIA-CIgG in the cell line 293 T by Co-IP. The plasmids pcDNA 3.1 and pEGFP-C3 were used as controls. Data are from one experiment that was representative of three (**a**–**h**) independent experiments with similar results. Also see Supplementary Figs. S4 and S5.

Purification of IgG from the TME

Ovarian cancer tissue samples or EMT-6 tumors implanted in NOD SCID mice were minced in liquid nitrogen and lysed in RIPA lysis buffer (10 mM Tris-HCL, pH 7.2; 1% Triton X-100; 1% sodium deoxycholate; 0.1% sodium dodecyl sulfate; and 0.15 M NaCl) containing a protease inhibitor cocktail (04693159001, Roche) at 4 °C for 30 min. The lysates were then centrifuged at 13,000 rpm for 30 min at 4 °C. The supernatants were collected, diluted with PBS and loaded onto a Protein G SepharoseTM 4 Fast Flow (17-0618-01, GE Healthcare) column, followed by incubation, washing and elution according to the manufacturer's recommendations. The eluted IgG from the TME was preserved in PBS with 10% maltose.

Purification of cancer-derived sialylated IgG

Cancer-derived sialylated IgG (SIA-CIgG) was purified either with agarose-bound *Sambucus nigra* Lectin (SNA) or RP215-coupled sepharose. IgG from the TME was loaded onto a SNA (AL-1303, Vector Laboratories) column to obtain sialylated Cancer-IgG according to the manufacturer's recommendations. The SIA-CIgG-specific antibody RP215 (generated by Prof. Lee) was coupled to CNBr-activated Sepharose™ 4B (71-7086-00 AF, GE Healthcare) according to the manufacturer's recommendations. IgG from the TME was incubated with the RP215-coupled CNBr-activated sepharose column for RP215 recognition-based SIA-CIgG purification.

Preparation of recombinant Cancer-IgG

Recombinant Cancer-IgG was constructed according to the predominant V_HDJ_H sequence V_H5-51/D3-16/J_H4 (GenBank: AY270190.1) and the $V_\kappa J_\kappa$ sequence V_κ4-1/J_κ3 (GenBank: AY505537.1) in human epithelial cancer cells, expressed in the CHO-K1 cell expression system and purified by Beijing Sino Biological Inc.

Neuraminidase digestion

IgG from the TME was combined with H_2O in a total reaction volume of 9 μl, and then 2 μl 10 × GlycoBuffer and 2 μl neuraminidase (P0720, New England Biolabs) or α2-3 neuraminidase (P0743S, New England Biolabs) were added and incubated at 37 °C for 1 h. For the control group, only GlycoBuffer was added.

Preparation of Fab and Fc fragments

Purified SIA-CIgG was treated according to the Pierce™ Fab Preparation Kit (44985 Pierce) recommendations. The Thermo Scientific™ Pierce™ Fab Preparation Kit enables efficient Fab generation from IgG. This kit uses papain, a nonspecific thiol endopeptidase, immobilized on agarose resin. Enzyme immobilization is advantageous because digestion can be immediately stopped by simply removing the IgG solution from the resin, resulting in a digest that is enzyme-free.

SDS-PAGE and western blotting

Purified IgG was denatured with heat, analyzed by 12.5% SDS-polyacrylamide gel electrophoresis (PAGE), and stained with Coomassie Brilliant Blue. For western blot analysis, proteins were transferred to nitrocellulose membranes. RP215, a goat anti-human IgG (gamma chain specific) polyclonal antibody (sc-34665, Santa Cruz), a goat anti-human Siglec-10 antibody (AF-2130, R&D), a rabbit anti-GFP antibody (50430-2-AP, Proteintech), a rabbit anti-Myc antibody (16286-1-AP, Proteintech), a mouse anti-His antibody (66005-1-Ig, Proteintech), and a rabbit anti-human IgG (Fc)-HRP antibody (SE205, Solarbio) were used as primary antibodies. After an incubation with secondary antibodies, including HRP-conjugated goat anti-mouse or rabbit anti-goat IgG antibodies (ZB-2301, ZB-2305, Beijing Zhongshan Golden Bridge Biotechnology), the blots were visualized by ECL chemiluminescence (32106, Pierce and RPN2235, GE). For sialylated IgG detection, the membranes were incubated with biotinylated SNA (B-1305, Vector Laboratories), MAL II (B-1265-1, Vector Laboratories) and IRDye 800-conjugated streptavidin (926-32230, LI-COR Biosciences) or horseradish peroxidase-labeled streptomycin (ZB-2404, Beijing Zhongshan Golden Bridge Biotechnology), and the signal was detected by the Odyssey Imaging System (LI-COR Bioscience).

Immunohistochemistry

Antigen retrieval was conducted by immersing slides in Tris-EDTA buffer (pH 9.0) at 120 °C for 2 min. The sections were incubated with 3% H_2O_2 for 10 min and blocked in 10% normal goat serum (ZLI-9056, Beijing Zhongshan Golden Bridge Biotechnology) at room temperature for 10 min. The sections were then incubated with the primary antibody RP215 overnight at 4 °C. After thorough washing, the sections were incubated with horseradish peroxidase (HRP)-conjugated anti-mouse IgG (GK500705, Dako) at room temperature for 20 min. The bound antibodies were detected using 0.05% DAB (Dako).

Cell proliferation

PBMCs, PBLs, and sorted B and T cells were suspended at a concentration of 5×10^6 cells/ml in PBS containing 5% FBS. Then, mouse T cells were blocked with anti-mouse CD16/CD32 antibodies (14-0161-82, eBioscience), and the cells were stained with CellTrace™ CFSE (C34554, Invitrogen) at a concentration of 5 μM and incubated at room temperature for 5 min. Staining was quenched by the addition of 10 ml PBS, and the cells were centrifuged at 1800 rpm for 5 min at 4 °C. The cells were washed twice in PBS, added to a 96-well plate, and stimulated by either 20 μg/ml PHA (00-4977-93, Thermo Fisher Scientific), precoated 3 μg/ml anti-CD3 antibody (OKT3; 317303, BioLegend) and 1 μg/ml anti-CD28 antibody (302913, BioLegend), or 20 μg/ml staphylococcal protein A (P7155 Sigma) or left unstimulated. Mouse T cells were stimulated with 5 μg/ml anti-CD3e antibody (145-2c11, 553057 BD Biosciences) and 2 μg/ml

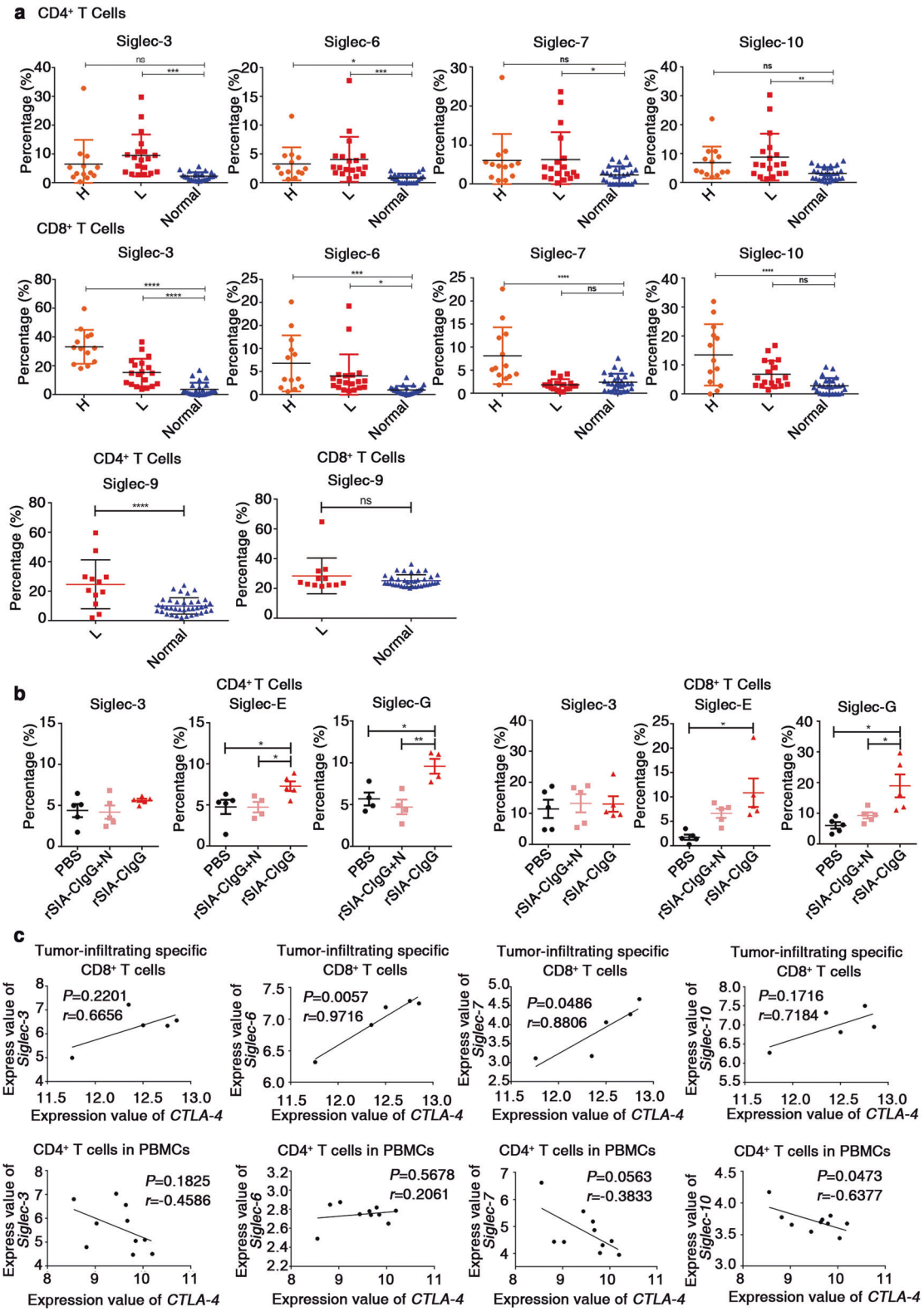

Fig. 7 Expression of Siglecs in effector T cells is elevated in patients with cancers, but not in healthy donors. **a** Frequencies of Siglec$^+$ cells among CD4$^+$ or CD8$^+$ T cells from the PBMCs of patients with cancer ($n = 13$ (head and neck cancer) and $n = 19$ (lung cancer)) or healthy donors ($n = 26$), as determined by flow cytometry. Frequencies of Siglec-9$^+$ cells among CD4$^+$ or CD8$^+$ T cells from the PBMCs of patients with cancer ($n = 19$ (lung cancer)) or healthy donors ($n = 37$), as determined by flow cytometry. H, head and neck cancer; L, lung cancer. **b** Proportions of Siglec-3-, Siglec-E-, and Siglec-G-expressing CD4$^+$ or CD8$^+$ T cells in EMT-6 tumors in mice treated with PBS, rSIA-ClgG, or rSIA-ClgG + N (20 μg, $n = 5$). N, neuraminidase. rSIA-ClgG, recombinant SIA-ClgG. **c** Correlations between the expression of *Siglec* and *CTLA-4* in GSE114944 (upper panel) and GSE36765 (lower panel). Each symbol represents an individual sample; small horizontal lines (**a**, **b**) indicate the mean (± s.d.). ns, not significant ($P \geq 0.05$); $^{*}P \leq 0.05$; $^{**}P \leq 0.01$; $^{***}P \leq 0.001$; and $^{****}P \leq 0.0001$ (one-way ANOVA followed by Tukey's multiple-comparisons test (**a**, **b**); two-tailed Pearson correlation for unpaired data (**c**)). Also see Supplementary Fig. S6.

anti-CD28 antibody (37.51, 553294 BD Biosciences) or left unstimulated. IgG from the TME, IVIG or the same volume of PBS was then added to the culture medium. In blocking experiments, 20 μg/ml anti-Siglec-7 (AF-1138, R&D), anti-Siglec-10 (AF-2130, R&D), or goat IgG antibody (ZDR-5005, Beijing Zhongshan Golden Bridge Biotechnology) was added 2 h before SIA-CIgG addition.

CCK8 assay

B16 cells were seeded in a 96-well plate at a density of 2×10^4 cells/well in 100 μL of culture medium with PBS, hTME-IgG, or IVIG. The cells were cultured in a CO_2 incubator at 37 °C for 0, 24, 48, or 72 h in the incubator. In total, 10 μL of CCK8 solution was added to each well of the plate using a repeating pipettor. The plate was incubated for 2 h in the incubator. The absorbance at 450 nm was measured using a microplate reader after testing cell proliferation.

Flow cytometry

Human PBMCs and mouse T cells were prepared as previously described and stained for 30 min at 4 °C with the following fluorophore-conjugated monoclonal antibodies obtained from eBioscience: anti-human CD4 (45-0048-41), CD8a (17-0087-41), CD19 (11-0199-41), Siglec-3 (12-0338-41), and Siglec-10 (347603) from BioLegend. Anti-mouse CD16/CD32 (14-0161-82, eBioscience), mouse IgG1K Isotype Control APC (17-4714-82, eBioscience), anti-mouse Siglec-G (17-5833-80, eBioscience), anti-mouse Siglec-E (677111, BioLegend), and anti-mouse Siglec-3 (CD33) (12-0331-80, eBioscience) were also obtained. For sialylated IgG binding detection, 40 μg/ml sialylated IgG was incubated with cells for 45 min at 4 °C, and the secondary antibody anti-human IgG Fc (12-4998-82, eBioscience) was added for 30 min at 4 °C. For Siglec-6, Siglec-7 and siglec-9 detection, anti-human Siglec-6 (MAB2859-SP, R&D Systems), Siglec-7 (AF-1138, R&D Systems), and Siglec-9 (1529365, R&D Systems) antibodies were incubated with cells for 45 min at 4 °C, and FITC-labeled goat anti-mouse IgG or rabbit anti-goat IgG antibodies (ZF-0312 or ZF-0314, Beijing Zhongshan Golden Bridge Biotech) were used as secondary antibodies and incubated for 30 min at 4 °C. Immune cells isolated from mouse draining lymph nodes and tumors with Percoll (P8370, Solarbio Life Science) were stained with anti-mouse CD4 (45-0042-80), CD8 (12-0081-81), CD19 (11-0191-82), CD11b (45-0112-82), CD45 (17-0451-82), Siglec-G (17-5833-80, eBioscience), Siglec-E (677111, BioLegend), and Siglec-3 (CD33) (12-0331-80, eBioscience) antibodies. Cells were collected on a FACSVerse or FACSCanto plus flow cytometer (BD Biosciences) and analyzed using FlowJo software.

RNA isolation and RT-PCR

The total RNA was extracted from PBMCs and mouse spleen or lymph node, sorted and stimulated $CD4^+$ and $CD8^+$ T cells using Trizol Reagent (15596018, Life Technology) or the Rapure Total RNA Mini Kit (R4011-02, Magen). Reverse transcription (RT) was carried out with the RevertAid First Stand cDNA Synthesis Kit (K1622, Thermo Fisher Scientific) according to the manufacturer's protocol. After the cDNA was obtained, specific primers were used to amplify the Siglec gene using the conditions described in Supplementary Tables S1 and S2.

GAPDH: Sense primer: CAAGGTCATCCATGACAACTTTG; and antisense primer: GTCCACCACCCTGTTGCTGTAG.

Coimmunoprecipitation analysis

The human Siglec-10 gene in the pcDNA 3.1 plasmid (gifted by Professor Yu) or a control vector was transfected into NCI-H520 cells using Lipofectamine 3000 Reagent (L3000001, Thermo Fisher Scientific). The cells were suspended in a lysis buffer containing 50 mM Tris-HCl, pH 8.0; 120 mM NaCl; 1% nonidet P-40 (NP-40); and a protease inhibitor cocktail. The lysates were incubated with antibodies at 4 °C overnight and with protein G agarose beads (17-0618-01, GE Healthcare) for 4 h. The antibodies used for immunoprecipitation were an anti-Siglec-10 antibody and RP215. A matched isotype IgG (goat IgG, ZDR-5005; mouse IgG, ZDR-5006, Beijing Zhongshan Golden Bridge Biotechnology) was used as a negative control. The mouse Siglec-E/G genes in the pcDNA 3.1 plasmid (gifted by Professor Yu), mouse Siglec-3 (CD33) gene in the pCMV3 plasmid (MG50172-CH, Sino Biological), human SIA-CIgG pEGFP-C3 plasmid (from Tang Jingshu) or a control vector was transfected into 293 T cells using PEI Reagent (23966, Polysciences, Inc). The cells (1×10^7) were washed two times with PBS and resuspended with 1 mL of ice-cold lysis buffer (50 mM Tris-HCl, pH 7.5; 150 mM NaCl; and 0.05% NP-40) containing appropriate protease inhibitors. The tube was centrifuged at $12{,}000\times g$ for 5 min at 4 °C, and the supernatant was transferred to another tube. Anti-Myc-tag mAb magnetic beads or Anti-GFP-tag mAb magnetic beads (M047-11, MBL; D153-11, MBL) were added as suggested into the supernatant prepared earlier. The sample was mixed well and incubated with gentle agitation for 1 h at 4 °C. The tube was placed on a magnetic rack (MBL; code no. 3190) for a few seconds. The supernatant was removed, 1 mL of cold wash buffer (50 mM Tris-HCl pH 7.5, 150 mM NaCl, 0.05% NP-40) was added, and the magnetic beads were resuspended. The tube was then placed on the magnetic rack for a few seconds, and the supernatant was removed. This process was repeated three times. The magnetic beads were resuspended in 30 μL of loading buffer and boiled for 10 min, and then the tube was placed on the magnetic rack for a few seconds. Then, the samples were analyzed by 12.5% SDS-polyacrylamide gel electrophoresis (PAGE) and western blotting.

In vivo experiments

C57BL/6 mice or nude mice were injected with 2×10^5 B16 cells, and BALB/c mice were injected with 2×10^5 EMT-6 cells subcutaneously in the armpits of both forelimbs. After 5–7 days, tumor volume was measured, and the mice were randomly allocated into three groups. Each group was injected subcutaneously around the tumors with 5 or 20 μg IgG TME or IVIG, 20 μg recombinant SIA-CIgG, 20 μg enriched SIA-CIgG, or SIA-CIgG digested with neuraminidase or papain, PBS or neuraminidase every other day. The mice were then killed and analyzed for tumor volume and weight and the proportions of immune cells in the draining lymph nodes (DLN) or tumor tissue.

Dataset collection and GEO analysis

Siglec gene expression was evaluated in 433 datasets containing 10,422 Affymetrix Human Genome U133 Plus 2.0 array samples from the Gene Expression Omnibus (GEO) database and in 455 datasets containing 3,929 mouse genome 430 2.0 arrays on the ImmuSort website (http://immusort.bjmu.edu.cn). An RNA-Seq dataset of tumor-infiltrated T cells in lung cancer patients in the GEO database (GSE90728) was downloaded, and Siglec expression was evaluated by calculating the Transcripts Per Kilobase Million (TPM) score. Siglec gene expression in arrays of peripheral blood T cells of patients with melanoma (GSE24536) or breast cancer (GSE36765), tumor-infiltrating T cells of patients with head and neck cancer (GSE114944), or tumor-infiltrating T cells of mice (GSE89477) were analyzed by GEO2R.

Statistics

All data were analyzed with GraphPad Prism software and are presented as the mean ± s.d. or s.e.m. Statistical significance was determined by a two-tailed paired or unpaired Student's *t* test or one-way analysis of variance (ANOVA) followed by Tukey's multiple-comparisons test, with significance levels of $^{*}P\le0.05$; $^{**}P\le0.01$; $^{***}P\le0.001$; $^{****}P\le0.0001$; and ns, not significant ($P\ge0.05$).

ACKNOWLEDGEMENTS

We would like to thank G. Lee (Andrology Lab, University of British Columbia Centre for Reproductive Health, Vancouver, BC V5Z 4H4, Canada) for developing RP215. We

thank Y. Yu (National Key Laboratory of Medical Immunology & Institute of Immunology, Second Military Medical University) for the human and mouse Siglec-10 plasmids. This work was supported by research grants to X. Qiu from the key support projects of the National Natural Science Foundation's major research program (91642206), major international cooperation projects of the National Natural Science Foundation (81320108020), research institute fund of the NHC Key Laboratory of Medical Immunology, Peking University (BMU2018JDJS010), the Science Technology and Innovation Committee of Shenzhen Municipality (JCYJ20170413141047772) and nonprofit central research institute fund of the Chinese Academy of Medical Sciences (2018PT31039).

AUTHOR CONTRIBUTIONS

Y.Z. and X.Q. initiated and designed the research; Z.W., Z.G., W.S., E.L., and L.X. performed the experiments and analyzed and interpreted the results; J.Z. and J.T. contributed to testing the specificity of RP215 and confirmed the epitope recognized by RP215; L.Z. and X.Y. purified SIA-ClgG; W.P. carried out the GEO database mining and analysis; X.S. performed cell sorting by flow cytometry; W.X. produced and purified RP215; Z.W., Z.G., and X.Q. wrote the paper; and L.X., H.C. and X.C. provided clinical specimens and clinical and pathological information.

ADDITIONAL INFORMATION

The online version of this article (https://doi.org/10.1038/s41423-019-0327-9) contains supplementary material.

Competing interests: The authors declare no competing interests.

REFERENCES

1. Nand, S. & Molokie, R. Therapeutic plasmapheresis and protein A immunoadsorption in malignancy: a brief review. *J. Clin. Apher.* **5**, 206–212 (1990).
2. Veltri, R. W., Kikta, V. A., Wainwright, W. H. & Sprinkle, P. M. Biologic and molecular characterization of the IgG serum blocking factor (SBF-IgG) isolated from sera of patients with EBV-induced infectious mononucleosis. *J. Immunol.* **127**, 320–328 (1981).
3. Affara, N. I. et al. B cells regulate macrophage phenotype and response to chemotherapy in squamous carcinomas. *Cancer Cell* **25**, 809–821 (2014).
4. Qiu, X. et al. Human epithelial cancers secrete immunoglobulin g with unidentified specificity to promote growth and survival of tumor cells. *Cancer Res.* **63**, 6488–6495 (2003).
5. Babbage, G., Ottensmeier, C. H., Blaydes, J., Stevenson, F. K. & Sahota, S. S. Immunoglobulin heavy chain locus events and expression of activation-induced cytidine deaminase in epithelial breast cancer cell lines. *Cancer Res.* **66**, 3996–4000 (2006).
6. Geng, L. Y. et al. Expression of SNC73, a transcript of the immunoglobulin alpha-1 gene, in human epithelial carcinomas. *World J. Gastroenterol.* **13**, 2305–2311 (2007).
7. Zhu, X. et al. Distinct regulatory mechanism of immunoglobulin gene transcription in epithelial cancer cells. *Cell Mol. Immunol.* **7**, 279–286 (2010).
8. Li, M. et al. Promotion of cell proliferation and inhibition of ADCC by cancerous immunoglobulin expressed in cancer cell lines. *Cell Mol. Immunol.* **9**, 54–61 (2012).
9. Li, X. et al. The presence of IGHG1 in human pancreatic carcinomas is associated with immune evasion mechanisms. *Pancreas* **40**, 753–761 (2011).
10. Liang, P. Y. et al. Overexpression of immunoglobulin G prompts cell proliferation and inhibits cell apoptosis in human urothelial carcinoma. *Tumour Biol.* **34**, 1783–1791 (2013).
11. Jiang, C. et al. Immunoglobulin G expression in lung cancer and its effects on metastasis. *PloS One* **9**, e97359 (2014).
12. Lee, G., Laflamme, E., Chien, C. H. & Ting, H. H. Molecular identity of a pan cancer marker, CA215. *Cancer Biol. Ther.* **7**, 2007–2014 (2008).
13. Lee, G. Cancer cell-expressed immunoglobulins: CA215 as a pan cancer marker and its diagnostic applications. *Cancer Biomark.* **5**, 137–142 (2009).
14. Tang, J. et al. Lung squamous cell carcinoma cells express non-canonically glycosylated IgG that activates integrin-FAK signaling. *Cancer Lett.* **430**, 148–159 (2018).
15. Kaneko, Y., Nimmerjahn, F. & Ravetch, J. V. Anti-inflammatory activity of immunoglobulin G resulting from Fc sialylation. *Science* **313**, 670–673 (2006).
16. Koch, M. A. et al. Maternal IgG and IgA antibodies dampen mucosal T helper cell responses in early life. *Cell* **165**, 827–841 (2016).
17. Colucci, M. et al. Sialylation of N-linked glycans influences the immunomodulatory effects of IgM on T cells. *J. Immunol.* **194**, 151–157 (2015).
18. Nimmerjahn, F. & Ravetch, J. V. The antiinflammatory activity of IgG: the intravenous IgG paradox. *J. Exp. Med* **204**, 11–15 (2007).
19. von Gunten, S. et al. IVIG pluripotency and the concept of Fc-sialylation: challenges to the scientist. *Nat. Rev. Immunol.* **14**, 349 (2014).
20. Schwab, I. & Nimmerjahn, F. Intravenous immunoglobulin therapy: how does IgG modulate the immune system? *Nat. Rev. Immunol.* **13**, 176–189 (2013).
21. Galeotti, C., Kaveri, S. V. & Bayry, J. IVIG-mediated effector functions in autoimmune and inflammatory diseases. *Int Immunol.* **29**, 491–498 (2017).
22. Padet, L. & Bazin, R. IVIg prevents the in vitro activation of T cells by neutralizing the T cell activators. *Immunol. Lett.* **150**, 54–60 (2013).
23. Bull, C., Heise, T., Adema, G. J. & Boltje, T. J. Sialic acid mimetics to target the sialic acid-siglec axis. *Trends Biochem. Sci.* **41**, 519–531 (2016).
24. Crocker, P. R., Paulson, J. C. & Varki, A. Siglecs and their roles in the immune system. *Nat. Rev. Immunol.* **7**, 255–266 (2007).
25. Nakamura, Y. et al. Expression of CD33 antigen on normal human activated T lymphocytes [letter]. *Blood* **83**, 1442–1443 (1994).
26. Nicoll, G. et al. Identification and characterization of a novel siglec, siglec-7, expressed by human natural killer cells and monocytes. *J. Biol. Chem.* **274**, 34089–34095 (1999).
27. Zhang, J. Q., Nicoll, G., Jones, C. & Crocker, P. R. Siglec-9, a novel sialic acid binding member of the immunoglobulin superfamily expressed broadly on human blood leukocytes. *J. Biol. Chem.* **275**, 22121–22126 (2000).
28. Ikehara, Y., Ikehara, S. K. & Paulson, J. C. Negative regulation of T cell receptor signaling by Siglec-7 (p70/AIRM) and Siglec-9. *J. Biol. Chem.* **279**, 43117–43125 (2004).
29. Bandala-Sanchez, E. et al. T cell regulation mediated by interaction of soluble CD52 with the inhibitory receptor Siglec-10. *Nat. Immunol.* **14**, 741–748 (2013).
30. Stanczak, M. A. et al. Self-associated molecular patterns mediate cancer immune evasion by engaging Siglecs on T cells. *J. Clin. Invest.* **128**, 4912–4923 (2018).
31. Barkal, A. A. et al. CD24 signalling through macrophage Siglec-10 is a target for cancer immunotherapy. *Nature* **572**, 392–396 (2019).
32. Li, Y. et al. Malignant ascite-derived extracellular vesicles inhibit T cell activity by upregulating Siglec-10 expression. *Cancer Manag. Res.* **11**, 7123–7134 (2019).
33. Toubai, T. et al. Siglec-G represses DAMP-mediated effects on T cells. *JCI Insight* **2**, 92293 (2017).
34. Yang, B. et al. Correlation of immunoglobulin G expression and histological subtype and stage in breast cancer. *PloS One* **8**, e58706 (2013).
35. Liao, Q. et al. Aberrant high expression of immunoglobulin G in epithelial stem/progenitor-like cells contributes to tumor initiation and metastasis. *Oncotarget* **6**, 40081–40094 (2015).
36. Sheng, Z. et al. Involvement of cancer-derived IgG in the proliferation, migration and invasion of bladder cancer cells. *Oncol. Lett.* **12**, 5113–5121 (2016).
37. Liu, Y. et al. Binding of the monoclonal antibody RP215 to immunoglobulin G in metastatic lung adenocarcinomas is correlated with poor prognosis. *Histopathology* **67**, 645–653 (2015).
38. Sheng, Z. et al. IgG is involved in the migration and invasion of clear cell renal cell carcinoma. *J. Clin. Pathol.* **69**, 497–504 (2016).
39. Prabagar, M. G., Choi, H. J., Park, J. Y., Loh, S. & Kang, Y. S. Intravenous immunoglobulin-mediated immunosuppression and the development of an IVIG substitute. *Clin. Exp. Med.* **14**, 361–373 (2014).
40. van de Bovenkamp, F. S., Hafkenscheid, L., Rispens, T. & Rombouts, Y. The Emerging Importance of IgG Fab Glycosylation in Immunity. *J. Immunol.* **196**, 1435–1441 (2016).
41. Bayry, J. et al. Inhibition of maturation and function of dendritic cells by intravenous immunoglobulin. *Blood* **101**, 758–765 (2003).
42. Zhou, J. Y., Oswald, D. M., Oliva, K. D., Kreisman, L. S. C. & Cobb, B. A. The glycoscience of immunity. *Trends Immunol.* **39**, 523–535 (2018).
43. Macauley, M. S., Crocker, P. R. & Paulson, J. C. Siglec-mediated regulation of immune cell function in disease. *Nat. Rev. Immunol.* **14**, 653–666 (2014).
44. Wang, P., Yang, Y., Han, W. & Ma, D. ImmuSort, a database on gene plasticity and electronic sorting for immune cells. *Sci. Rep.* **5**, 10370 (2015).
45. Deng, J. et al. CDK4/6 inhibition augments antitumor immunity by enhancing T-cell activation. *Cancer Disco.* **8**, 216–233 (2018).
46. Kimoto, Y. Expression of heavy-chain constant region of immunoglobulin and T-cell receptor gene transcripts in human non-hematopoietic tumor cell lines. *Genes Chromosomes Cancer* **22**, 83–86 (1998).
47. Zheng, J. et al. Immunoglobulin gene transcripts have distinct VHDJH recombination characteristics in human epithelial cancer cells. *J. Biol. Chem.* **284**, 13610–13619 (2009).
48. Lv, W. Q. et al. Expression of cancer cell-derived IgG and extra domain A-containing fibronectin in salivary adenoid cystic carcinoma. *Arch. Oral. Biol.* **81**, 15–20 (2017).
49. Ji, F. et al. Prognostic value and characterization of the ovarian cancer-specific antigen CA166-9. *Int J. Oncol.* **47**, 1405–1415 (2015).
50. Rodrigues, E. & Macauley, M. S. Hypersialylation in cancer: modulation of inflammation and therapeutic opportunities. *Cancers* **10**, E207 (2018).
51. Wang, J. et al. Siglec-15 as an immune suppressor and potential target for normalization cancer immunotherapy. *Nat. Med.* **25**, 656–666 (2019).